Warsaw University of Technology

Highlights from the STAR experiment

Hanna Zbroszczyk

for the STAR Collaboration

Faculty of Physics, Warsaw University of Technology

MESON 2018, Kraków, 9th June 2018

Introduction

Relativistic Heavy Ion Collider (RHIC)
Brookhaven National Laboratory (BNL), New York

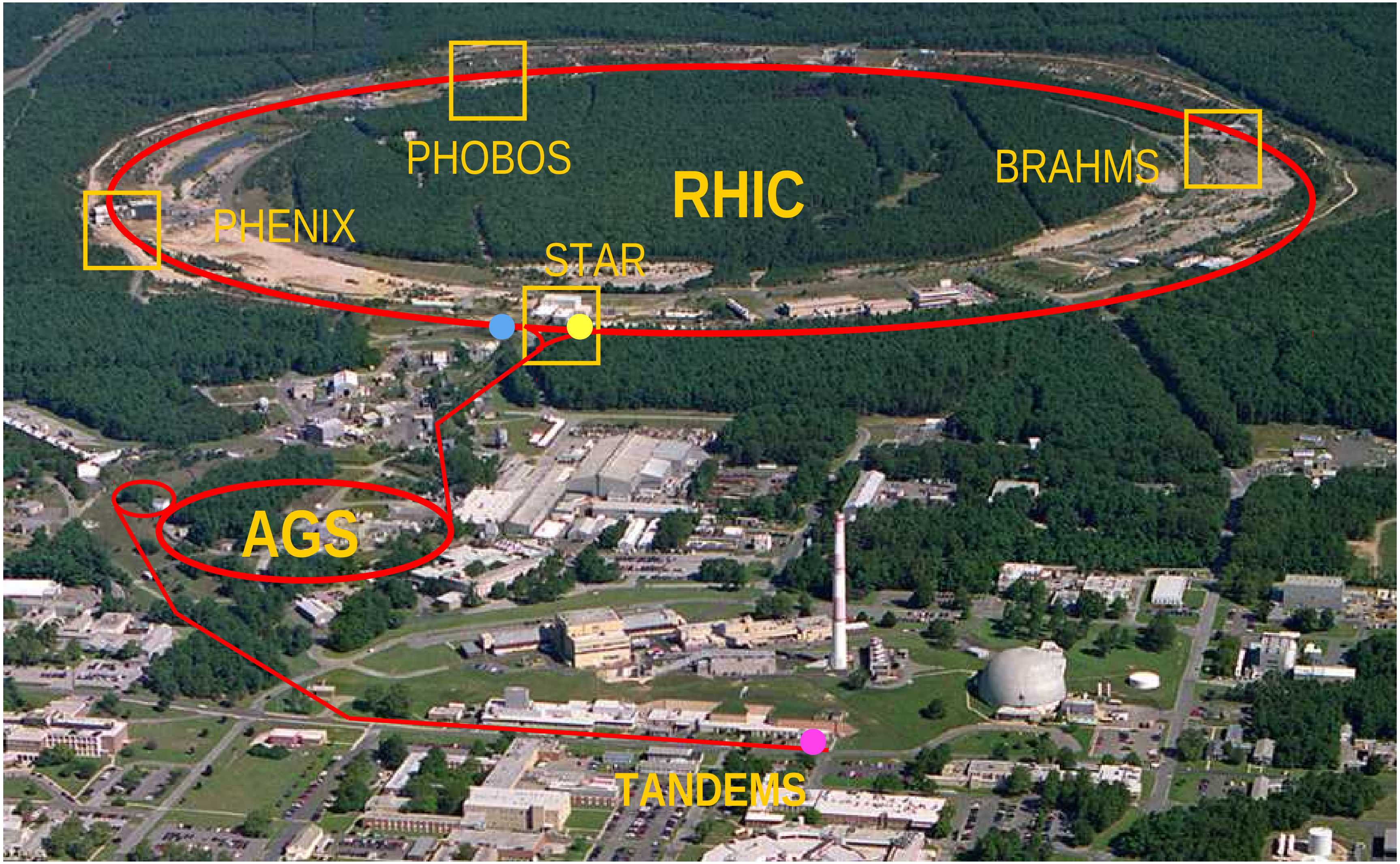

- 2 concentric rings of 1740 superconducting magnets
- 3.8 km circumference

The Solenoidal Tracker At RHIC

- **Tracking and PID (full 2π)**
  TPC: $|\eta| < 1$
  TOF: $|\eta| < 1$
  BEMC: $|\eta| < 1$
  EEMC: $1 < \eta < 2$
  HFT (2014-2016): $|\eta| < 1$
  MTD (2014+): $|\eta| < 0.5$

- **MB trigger and event plane reconstruction**
  BBC: $3.3 < |\eta| < 5$
  EPD (2018+): $2.1 < |\eta| < 5.1$
  FMS: $2.5 < \eta < 4$
  VPD: $4.2 < |\eta| < 5.1$
  ZDC: $6.5 < |\eta| < 7.5$

- **On-going/future upgrades**
  iTPC (2019+): $|\eta| < 1.5$
  eTOF (2019+): $-1.6 < \eta < -1$
  FCS (2021+): $2.5 < \eta < 4$
  FTS (2021+): $2.5 < \eta < 4$

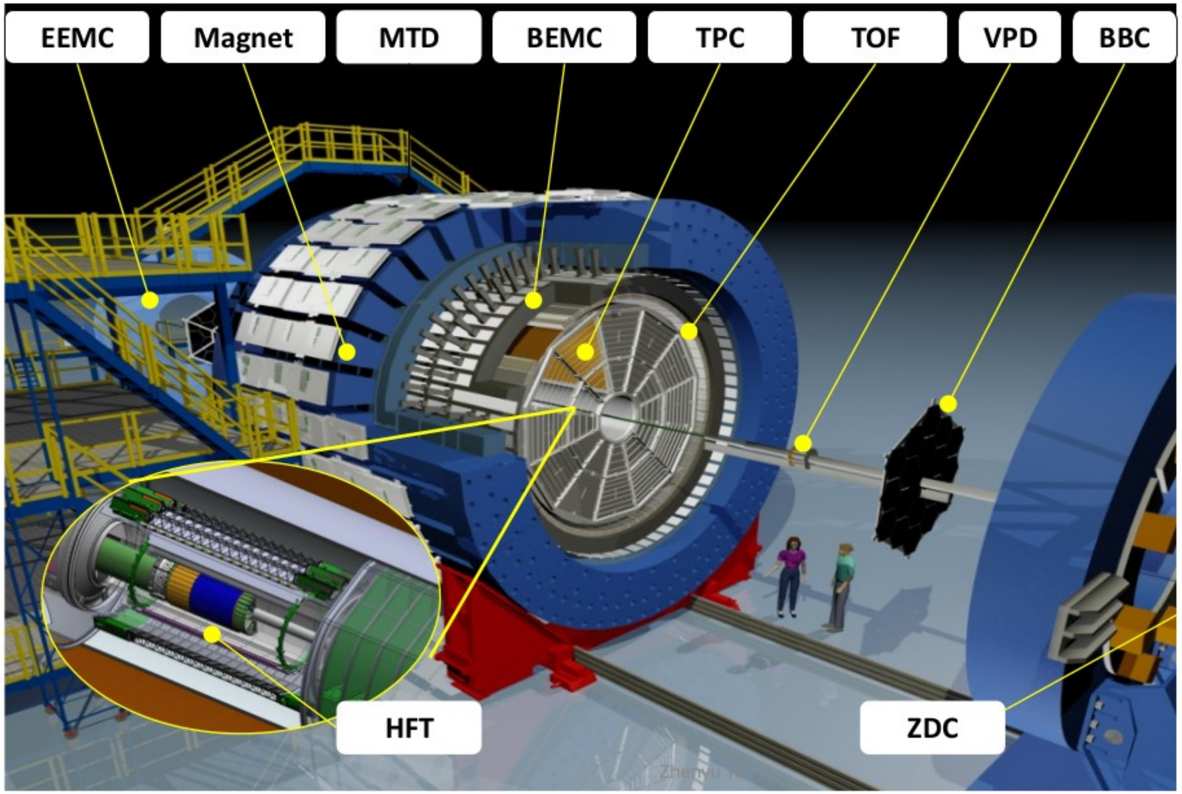

Introduction

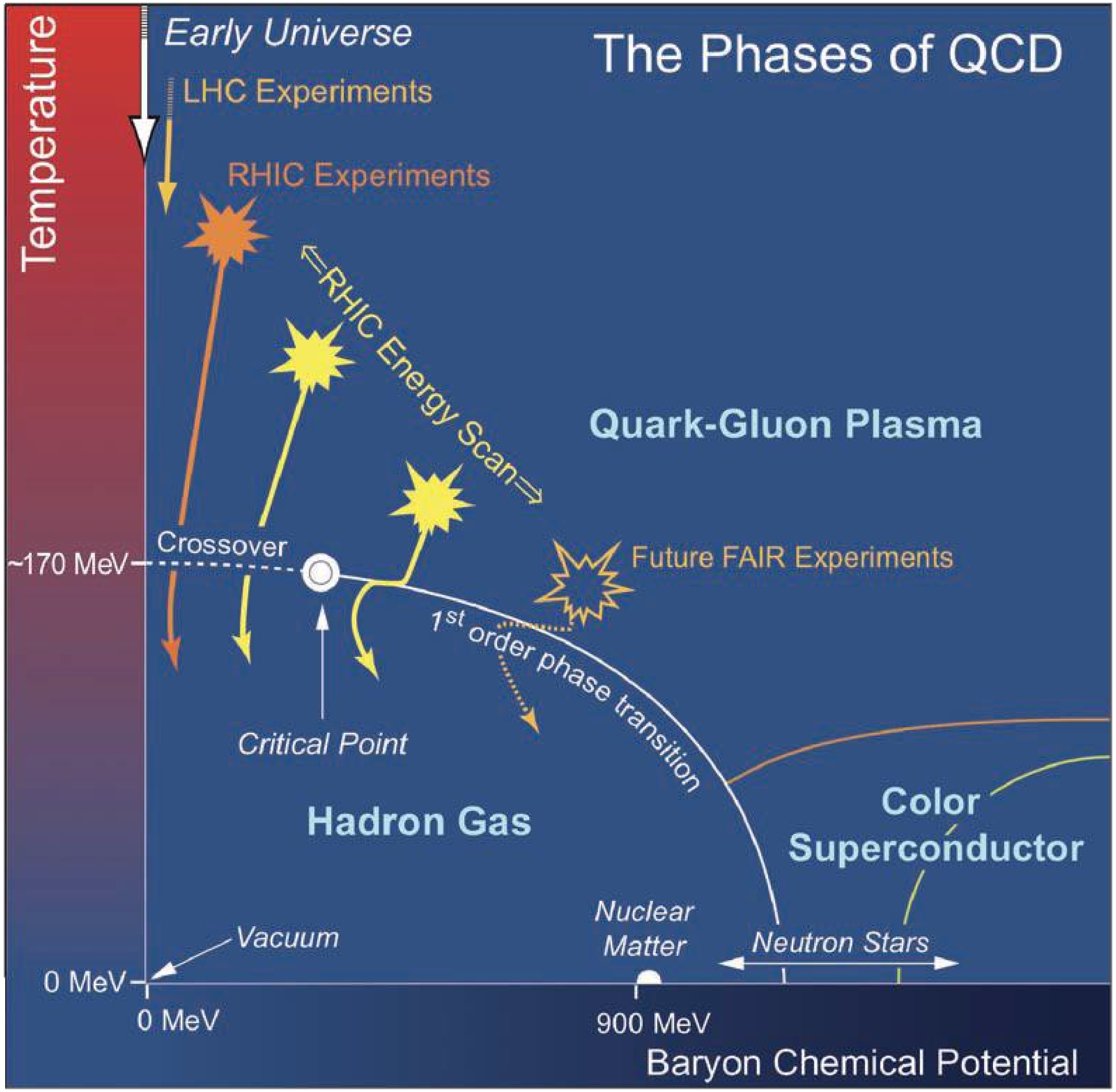

RHIC Top Energy

p+p, p+Al, p+Au, d+Au, ^{3}He+Au, Cu+Cu, Cu+Au, Ru+Ru, Zr+Zr, Au+Au, U+U

QCD at high energy density/temperature

Properties of QGP, EoS

Beam Energy Scan

Au+Au 7.7-62 GeV

QCD phase transition

Search for critical point

Turn-off of QGP signatures

Fixed-Target Program

Au+Au =3.0-7.7 GeV

High baryon density regime with 420-720 MeV

Introduction

1. Open heavy flavor - D^0 v_1, D^0 R_{AA} and R_{CP}, Λ_C

2. Quarkonium – Υ R_{AA}

3. Jet modification and high-p_T hadrons - di-jet imbalance, di-hadron correlation

4. Chirality, vorticity and polarization effects - Λ polarization, Φ polarization, CME, CMW

5. Initial state physics and approach to equilibrium - v_2 and v_3 fluctuations

6. Collectivity in small systems - v_2 in p+Au and d+Au

7. Collective dynamics - longitudinal decorrelation, identified particle v_1

8. High baryon density and astrophysics - v_1 from fixed target

9. Correlations and fluctuations – femtoscopy

10. Phase diagram and search for the critical point - net Λ and off-diagonal cumulants

11. Thermodynamics and hadron chemistry - triton, hypertriton mass

12. Upgrades - BES-II and forward upgrades

Introduction

1. Open heavy flavor - D^0 v_1, D^0 R_{AA} and R_{CP}, Λ_C

2. Quarkonium – Υ R_{AA}

3. Jet modification and high-p_T hadrons - di-jet imbalance, di-hadron correlation

4. Chirality, vorticity and polarization effects - Λ polarization, Φ polarization, CME, CMW

2. Initial state physics and approach to equilibrium - v_2 and v_3 fluctuations

3. Collectivity in small systems - v_2 in p+Au and d+Au

7. Collective dynamics - longitudinal decorrelation, identified particle v_1

4. High baryon density and astrophysics - v_1 from fixed target

5. Correlations and fluctuations – femtoscopy

10. Phase diagram and search for the critical point - net Λ and off-diagonal cumulants

6. Thermodynamics and hadron chemistry - triton, hypertriton mass

7. Upgrades - BES-II and forward upgrades (as summary)

Results

1) D^0 – Open heavy flavor

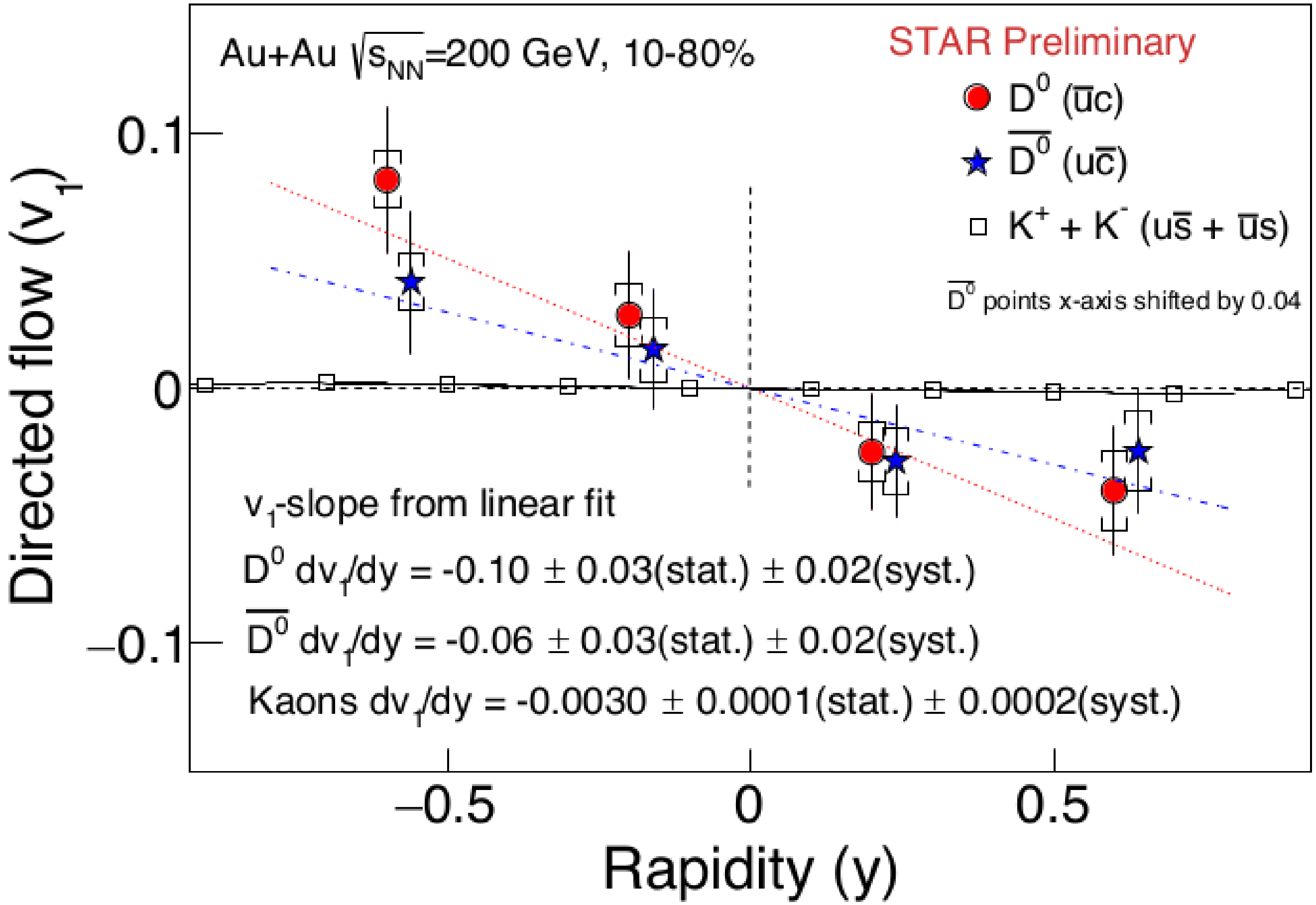

First evidence of non-zero D^0 v_1 is measured.

Probe the initial tilt of the source and the initial EM field

2) Initial state physics

Q-cumulant method (traditional)

$$\langle 2 \rangle_n = \left\langle e^{in(\phi_1 - \phi_2)} \right\rangle \qquad \langle 4 \rangle_{nm} = \left\langle e^{in(\phi_1 - \phi_2) + im(\phi_3 - \phi_4)} \right\rangle$$

$$v_n^4\{4\} = \langle 4 \rangle_{nn} - 2\,\langle 2 \rangle_n \langle 2 \rangle_n \qquad NSC(n,m) = \frac{\langle 4 \rangle_{nm} - \langle 2 \rangle_n \langle 2 \rangle_m}{\langle 2 \rangle_n^{Sub} \langle 2 \rangle_m^{Sub}}$$

Φ - azimuthal angle

Two-subevent method

$$\langle 2 \rangle_n^{Sub} = \left\langle e^{in(\phi_A - \phi_B)} \right\rangle \qquad v_n^2\{2\} = c_n\{2\} = \langle 2 \rangle_n^{Sub}$$

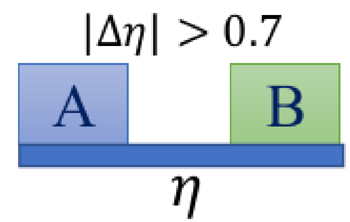

✓ Short-range non-flow contribution in $v_2\{2\}$ is suppressed by $|\Delta\eta| > 0.7$

$$v_n^4\{4\} = 2\langle v_n^2 \rangle^2 - \langle v_n^4 \rangle \qquad \left[\frac{v_n\{4\}}{v_n\{2\}}\right]^4 = 2 - \frac{\langle v_n^4 \rangle}{\langle v_n^2 \rangle^2}$$

Sensitive to flow fluctuations

2) Initial state physics

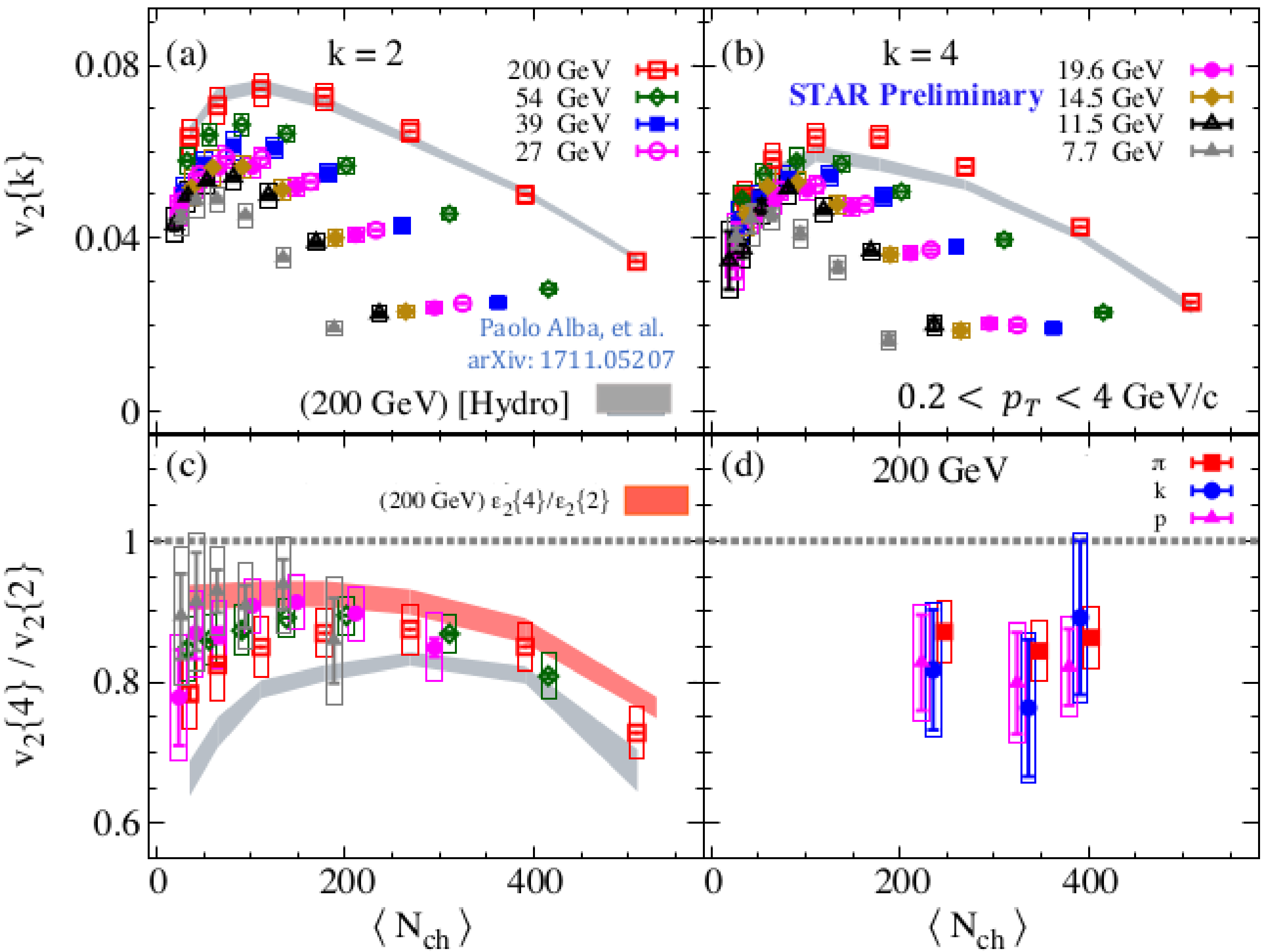

Strong dependence of $v_2\{k\}$ on collision energy.

Weak dependence of $v_2\{4\}/v_2\{2\}$ on collision centrality

2) Initial state physics

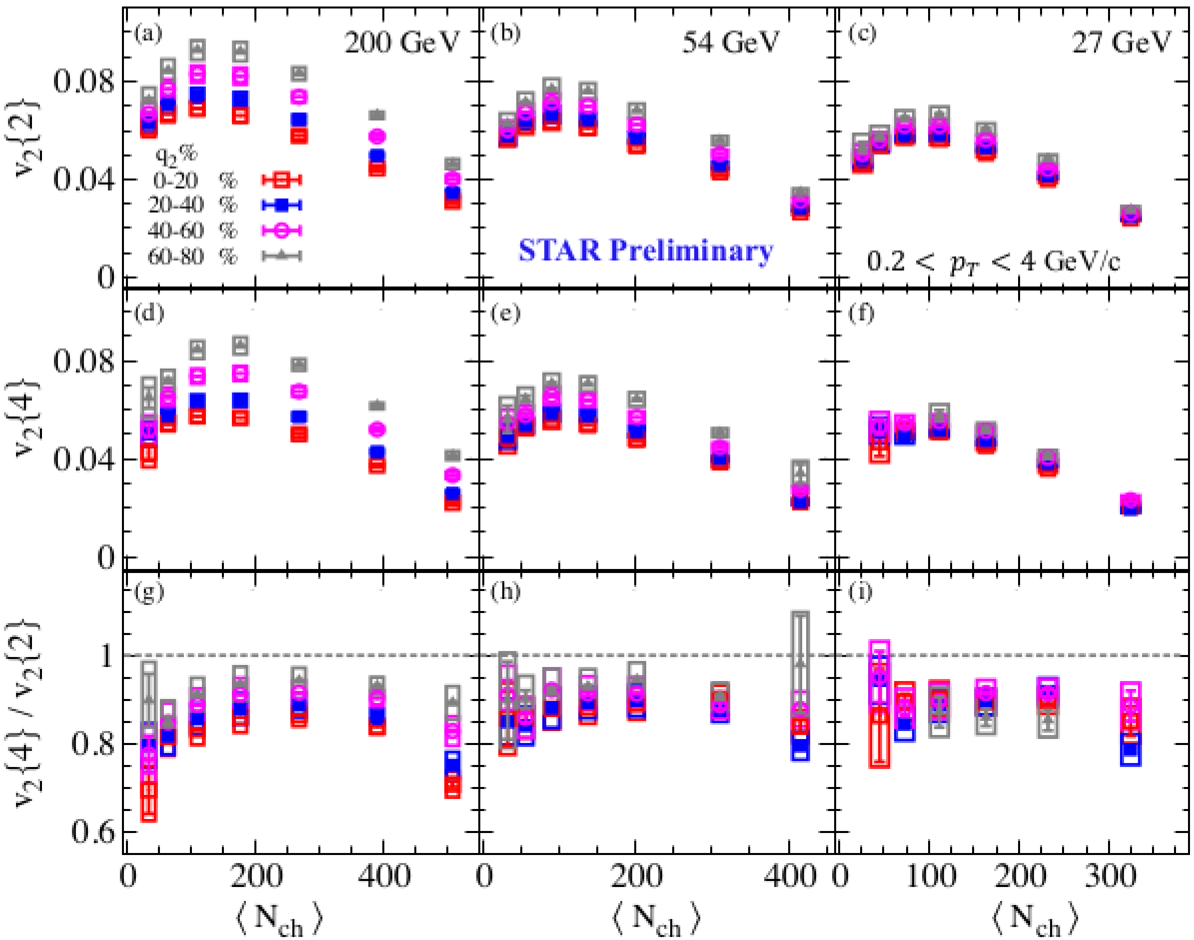

Strong dependence of $v_2\{2\}$ and $v_2\{4\}$ on collision centrality.

Weak dependence of $v_2\{2\}/v_2\{4\}$ on collision centrality

2) Initial state physics

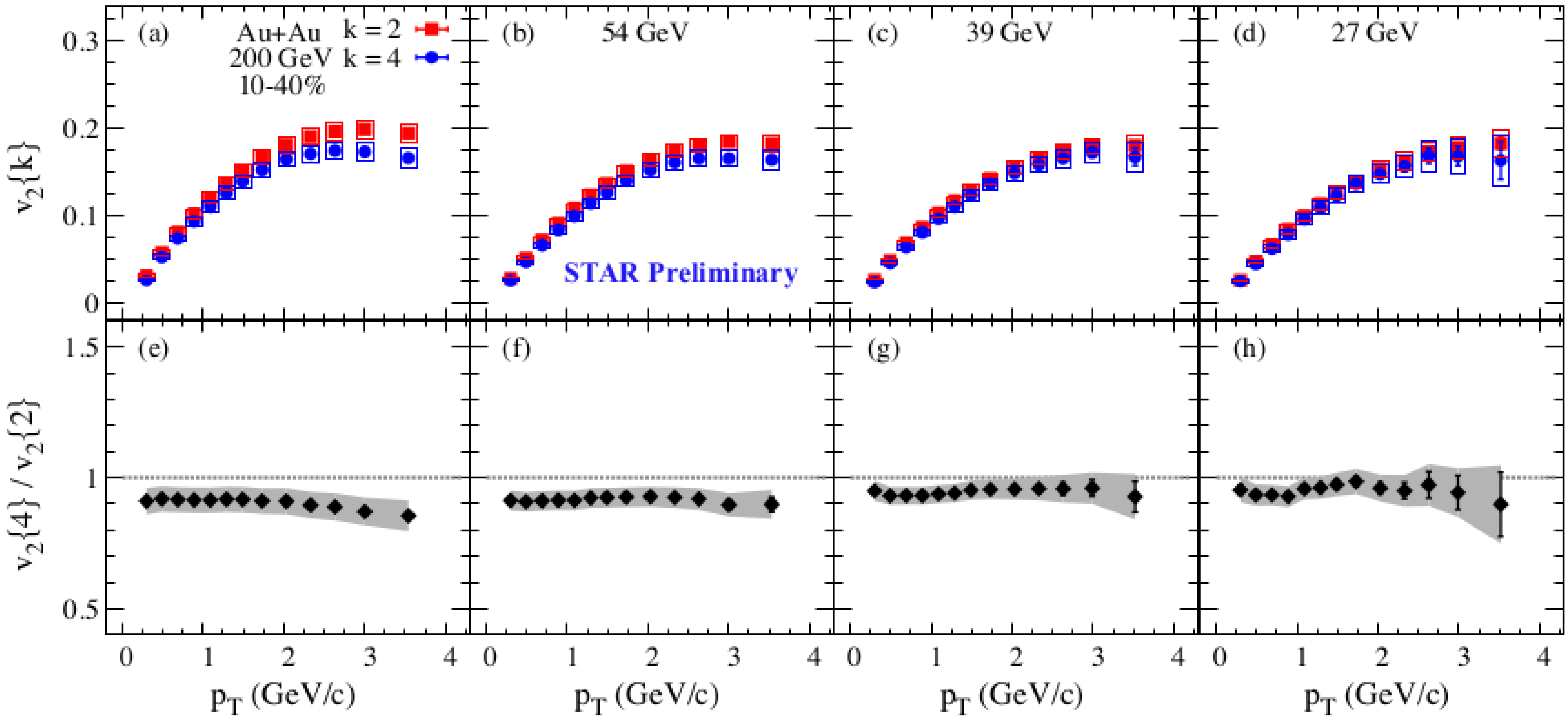

Weak dependence of $v_2\{2\}/v_2\{4\}$ on transverse momentum

2) Initial state physics

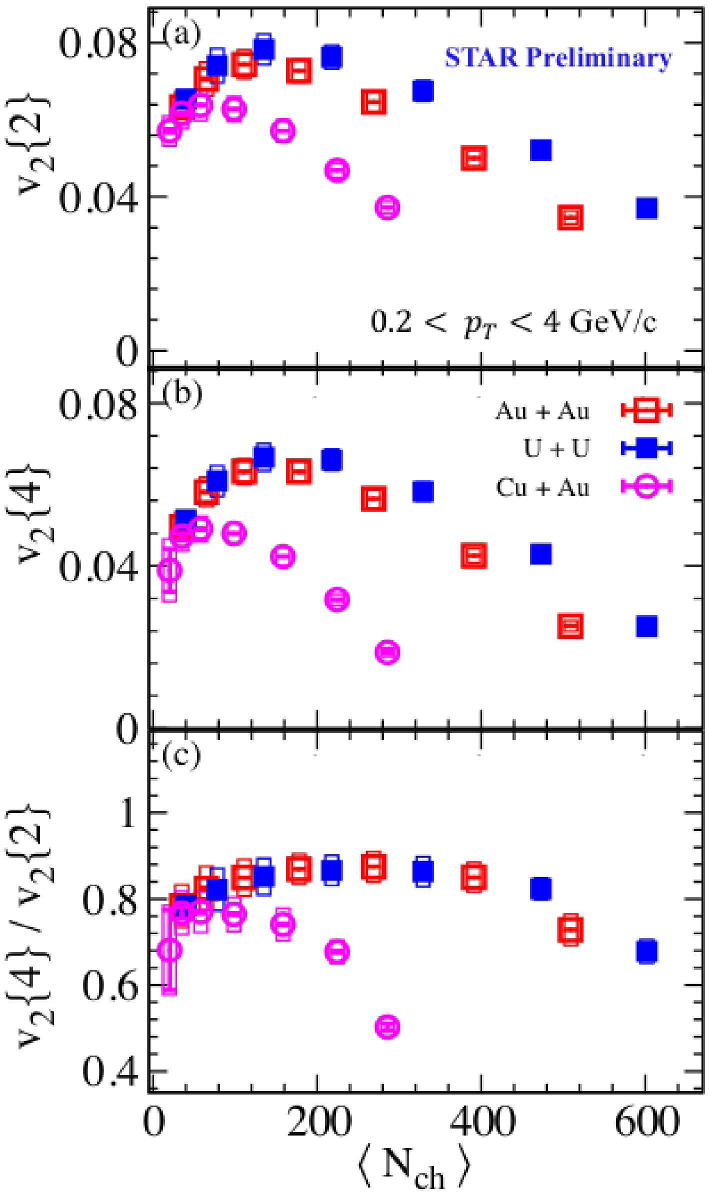

Significant dependence of $v_2\{2\}$, $v_2\{4\}$ and $v_2\{2\}/v_2\{4\}$ on $<N_{ch}>$ among different systems

2) Initial state physics

Anisotropic flow magnitude is sensitive to:
- initial-state spatial anisotropy
- flow fluctuations and correlations
- viscous attenuation ($\propto \eta/s\ (T)$)

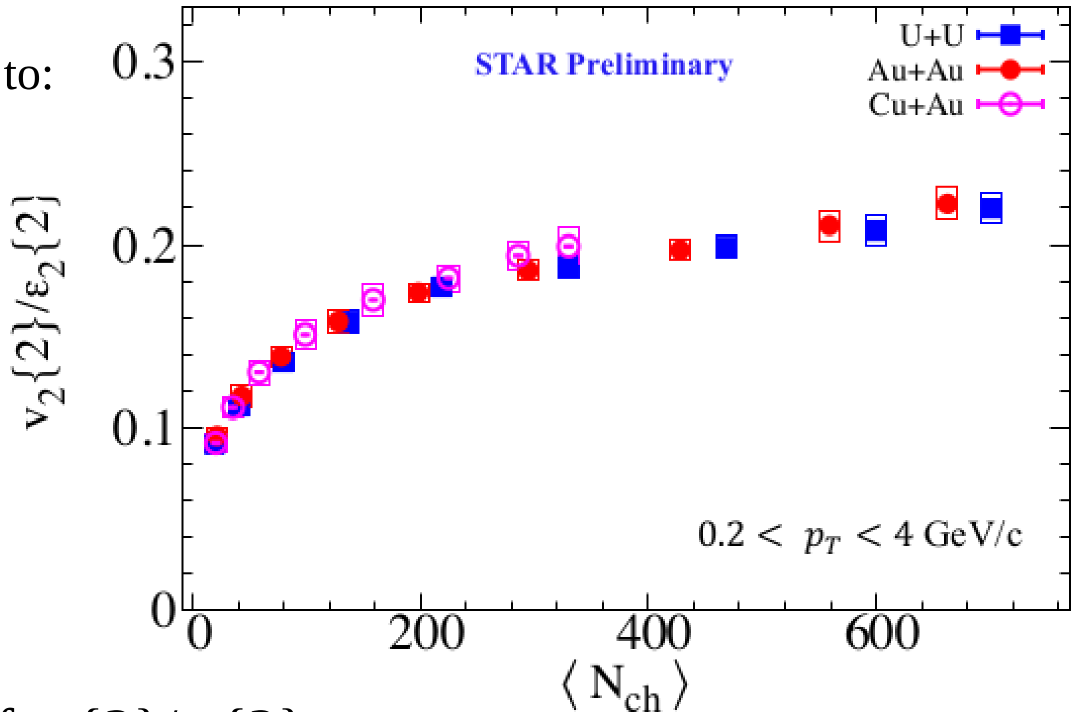

Weak dependence of $v_2\{2\}/\varepsilon_2\{2\}$ on collision centrality among different systems.

Are dynamical final-state fluctuations significantly less than the initial-state fluctuations?

2) Initial state physics

Strong dependence of $v_2\{2\}$, $v_2\{4\}$ on collision centrality, collision energy, transverse momentum

Weak dependence of $v_2\{4\}/v_2\{2\}$ and $v_2\{2\}/\varepsilon_2\{2\}$ (elliptic flow fluctuations) on the size of colliding system and:
collision centrality, collision energy, transverse momentum

Flow flucuations are dominated by the fluctuations of the **initial state eccentricity**

Similar viscous coefficient for different colliding systems

3) Small systems

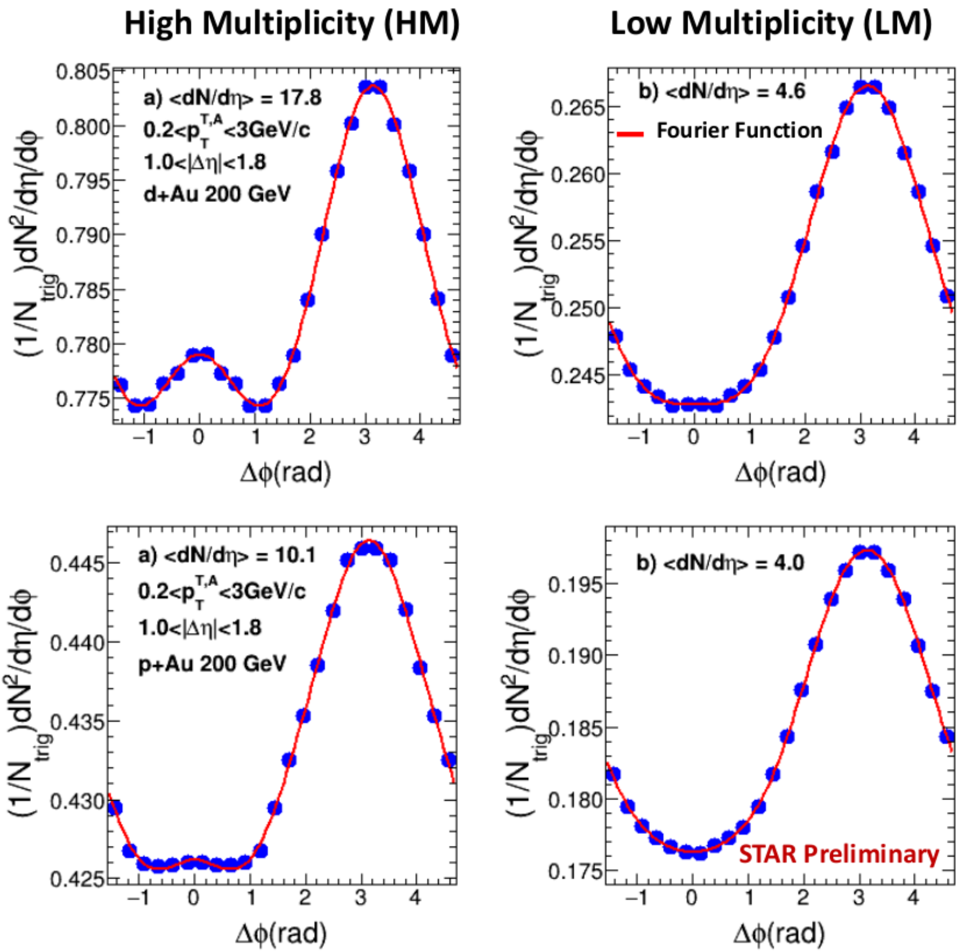

d+Au 200 GeV

p+Au 200 GeV

Near-side ridge observed in High Multiplicity (HM) of d+Au collisions

$$dN/d\Delta\phi \sim 1 + \sum_{n=1}^{4} 2V_{n,n} \times \cos(n\Delta\phi))$$

Integral $v_n = \mathrm{sqrt}(V_{n,n})$; $v_n(p_T) = V_{n,n}(p_T)/v_n$

3) Small systems

Low multiplicity subtraction scaled by short-range near-side (|Δη|<0.5) jet yield

$$V_{n,n}^{HM}(subtracted) = V_{n,n}^{HM} - V_{n,n}^{LM} \times \frac{N_{asso.}^{LM}}{N_{asso.}^{HM}} \times \frac{Y_{jet,near-side}^{HM}}{Y_{jet.near-side}^{LM}}$$

ATLAS:PRC90(2014)044906
CMS:PLB765(2017)193
STAR: PLB743(2015)333

Short-range near-side jet modification = long-range away-side jet modification

Template fit

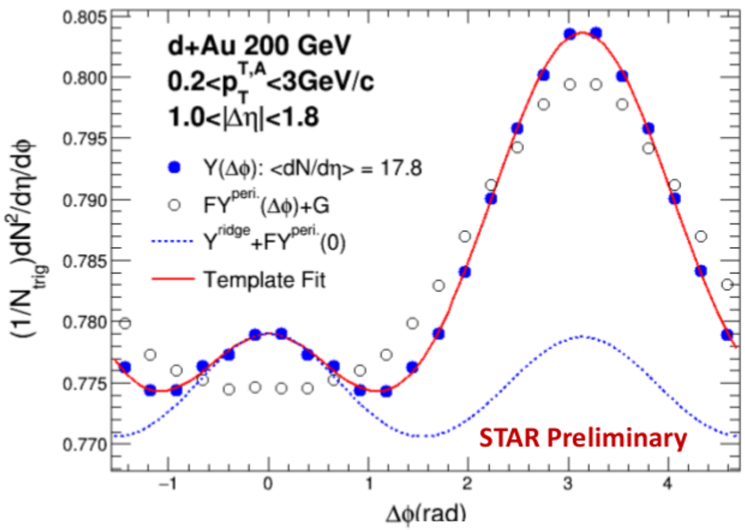

$$Y_{templ.}(\Delta\phi) = \mathrm{F} \times Y_{LM}(\Delta\phi) + Y_{ridge}(\Delta\phi)$$

where

$$Y_{ridge}(\Delta\phi) = \mathrm{G} \times (1 + 2 \times \sum_{n=2}^{4} V_{n,n} \times \cos(n\Delta\phi))$$

ATLAS:PRL(116)172301

A new method by ATLAS Collaboration away-side jet shape can be measured in Low Multiplicity (LM) events scaled by ”F” parameter
(due to jet modification)

3) Small systems

v_2 without subtraction is **larger** than that with subtraction for both methods.

The subtraction of non-flow contributions are very **important** for STAR results are comparable with PHENIX results.

At lowet p_T v_2 from Low Multiplicity subtraction is **35% lower** than from template fit

At intermediate p_T they **agree** with each other

STAR results are **comparable** with PHENIX ones.

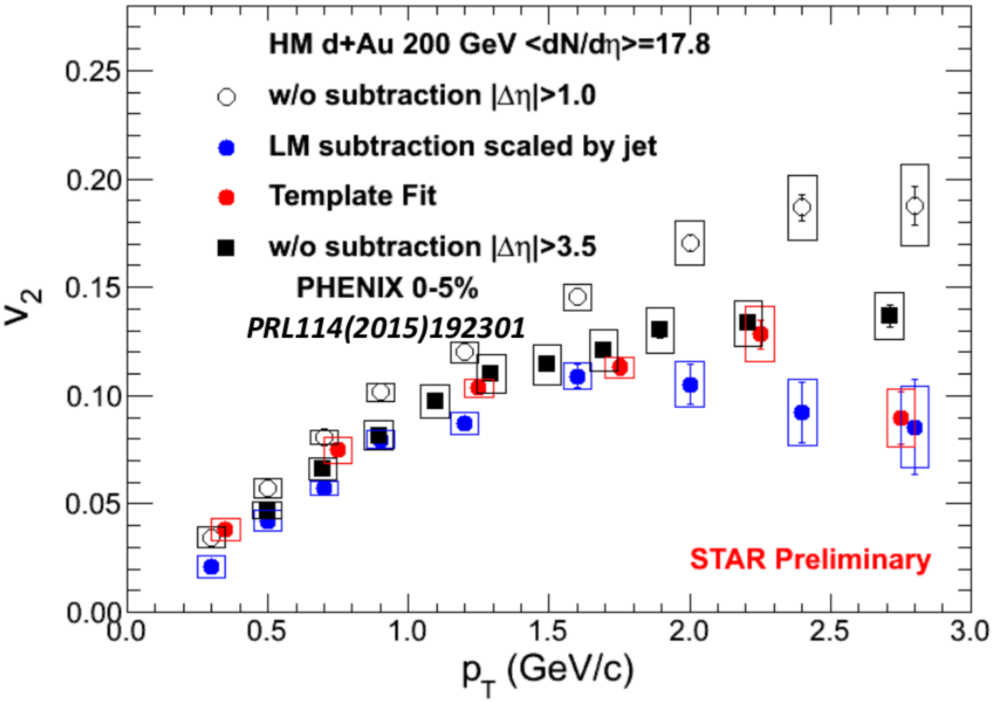

3) Small systems

v_2 in p+Au collisions without subtraction is **larger** than v_2 in d+Au collisions that with subtraction for both methods.

v_2 in p+Au collisions from Low Multiplicity subtraction is **lower** than from template fit.

STAR results are **comparable** with PHENIX results, except at high pT. The STAR data is clearly lower than PHENIX for p_T>1.5 GeV/c

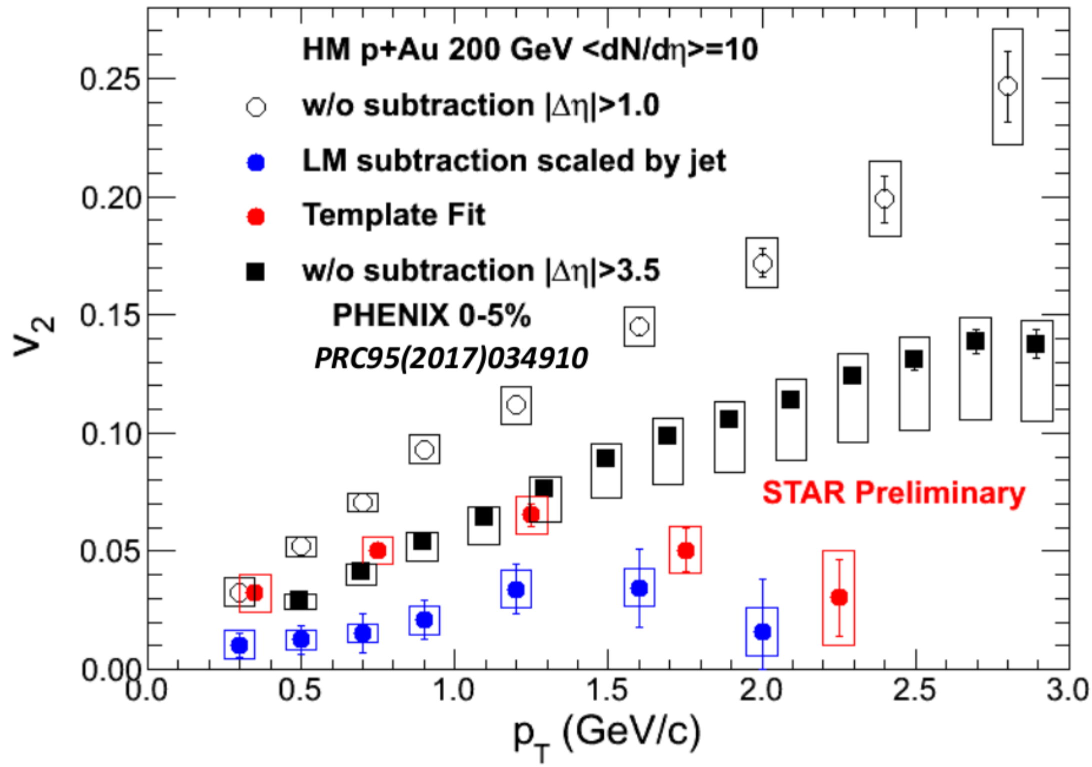

3) Small systems

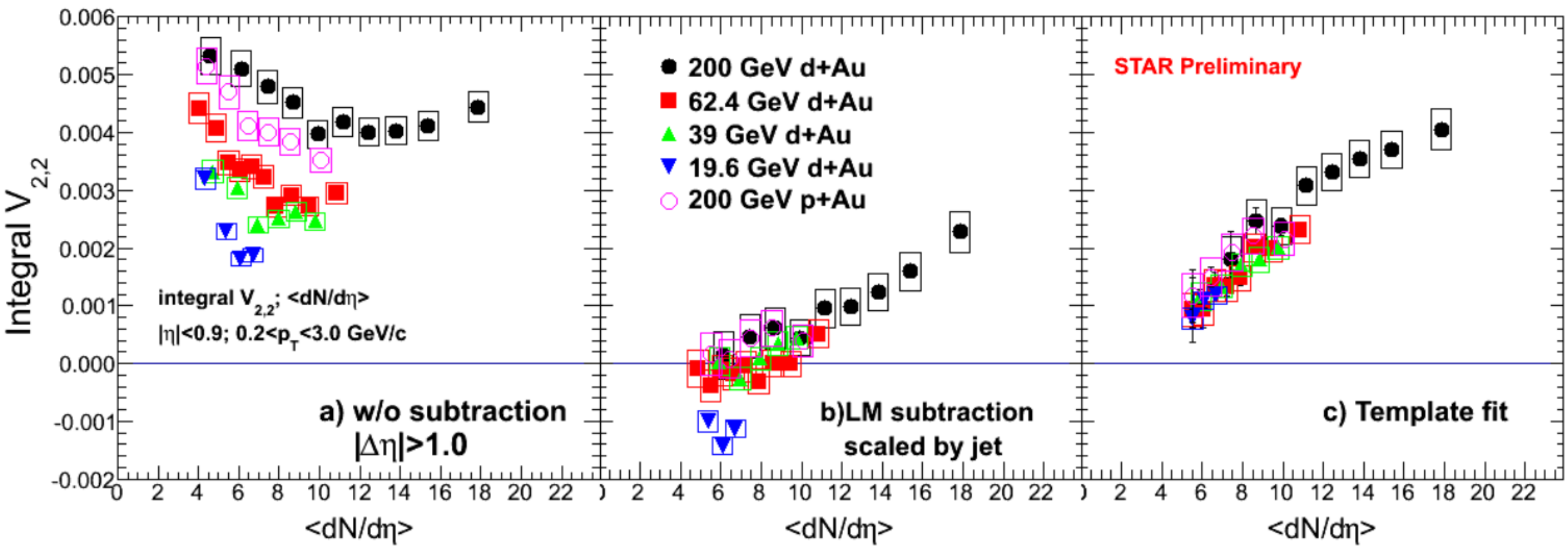

Large **difference** between subtraction method and template fit

v_2 from subtraction method is **negative** at lower collision energies (different kinematics between near-side and away-side jet-like correlations?)

v_2 from template fit **increases** with collision centrality

3) Small systems

v_2 becomes **negative** at high transverse momentum in d+Au collisions at low collision energy

The correlation from away-side jet is **stronger** at high transverse momentum

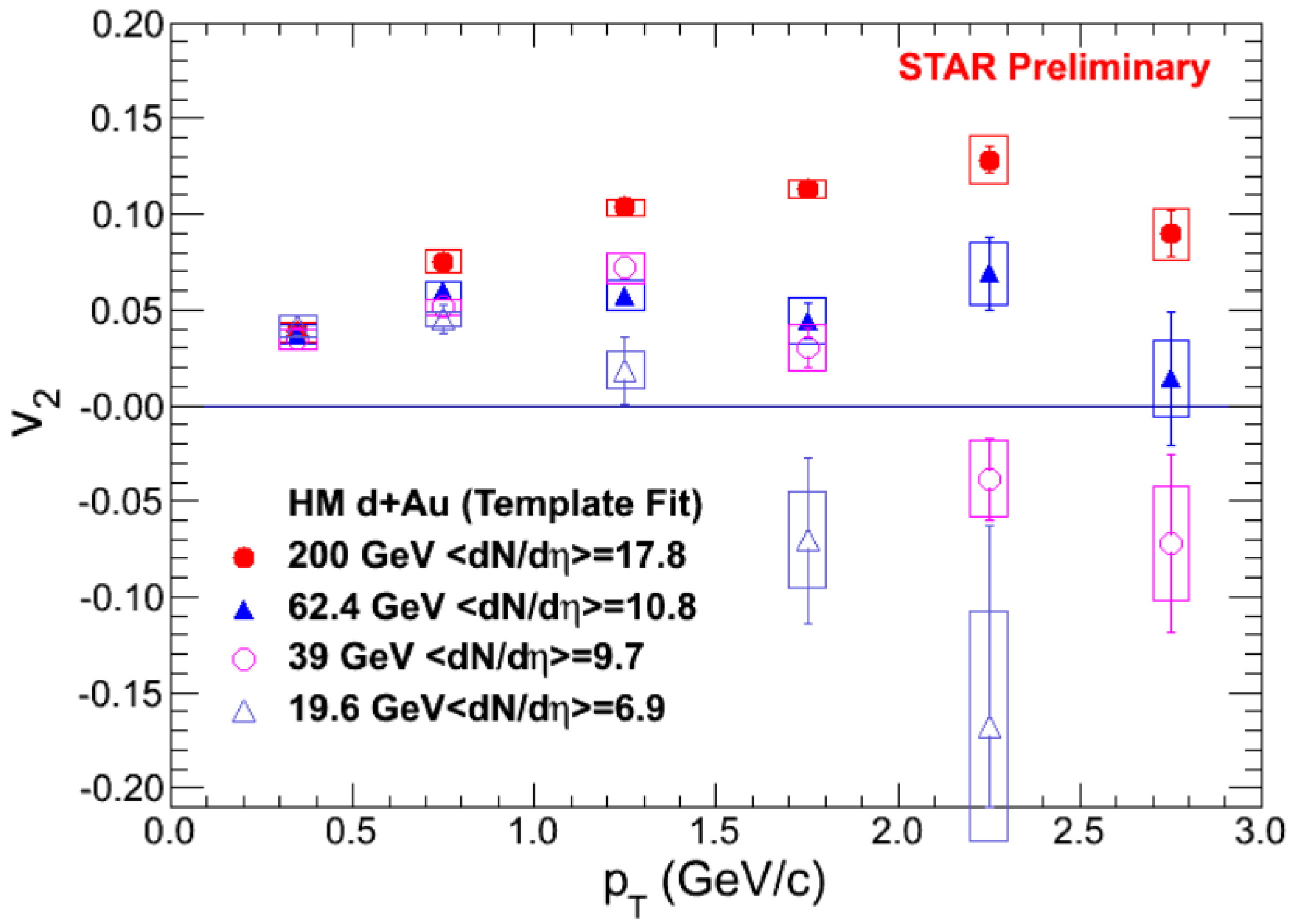

3) Small systems

Large **difference** between v_2 from two methods has been observed at low energy → large uncertainties in the non-flow subtraction in small systems.

We do see **similar v_2** between p+Au and d+Au collisions for same multiplicity → v_2 is not only driven by initial geometry.

The integral v_2 extracted by a template fit shows an **universal** trend as a function of $\langle dN/d\eta \rangle$ for different small systems at different energies → multiplicity plays an important role in small systems.

4) Fixed target mode

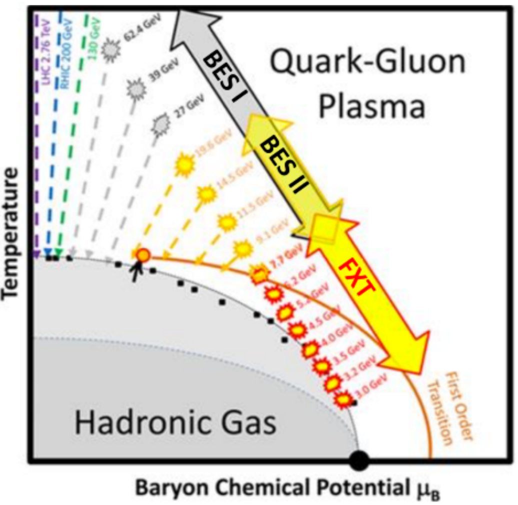

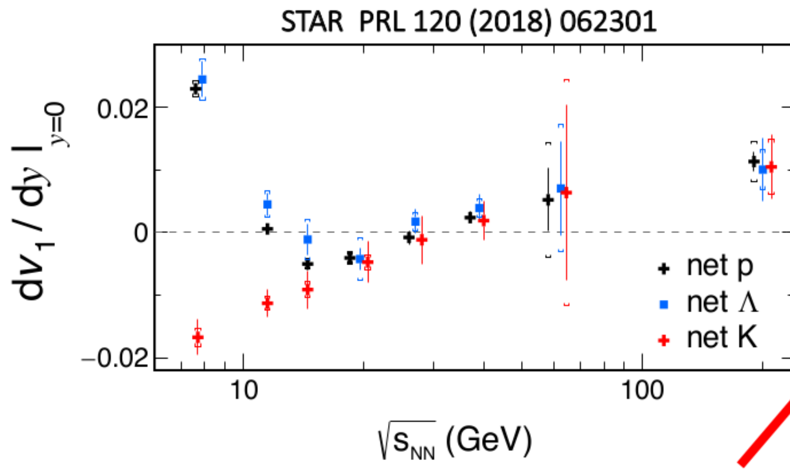

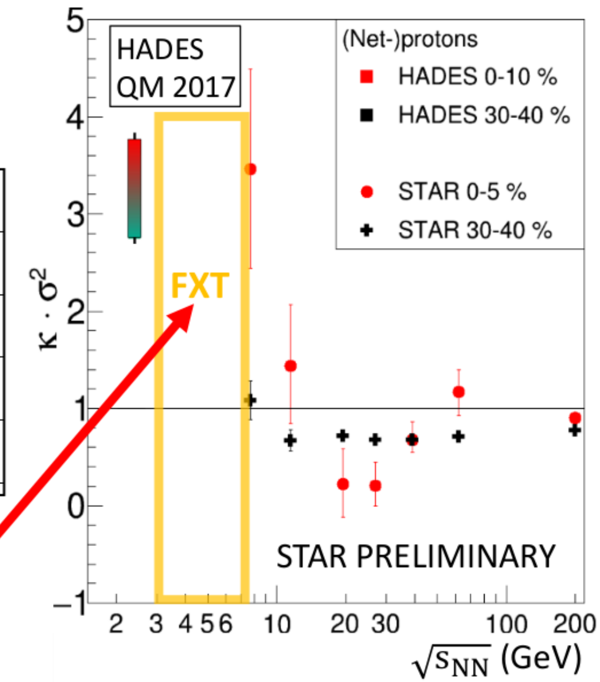

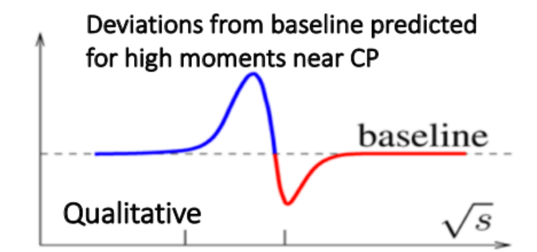

I. Stephanov J Phys G: Nucl Part Phys 38 (2011) 124147

BES goals:
- Search for 1st order phase transition
- Search for existance of the Critical Point
- Search for turn-off QGP signatures

Collider mode is unusable for $\sqrt{s_{NN}}$<7.7 GeV

Fix target mode is able to cover $\sqrt{s_{NN}}$ from 3.0 GeV to 7.7 GeV

4) Fixed target mode

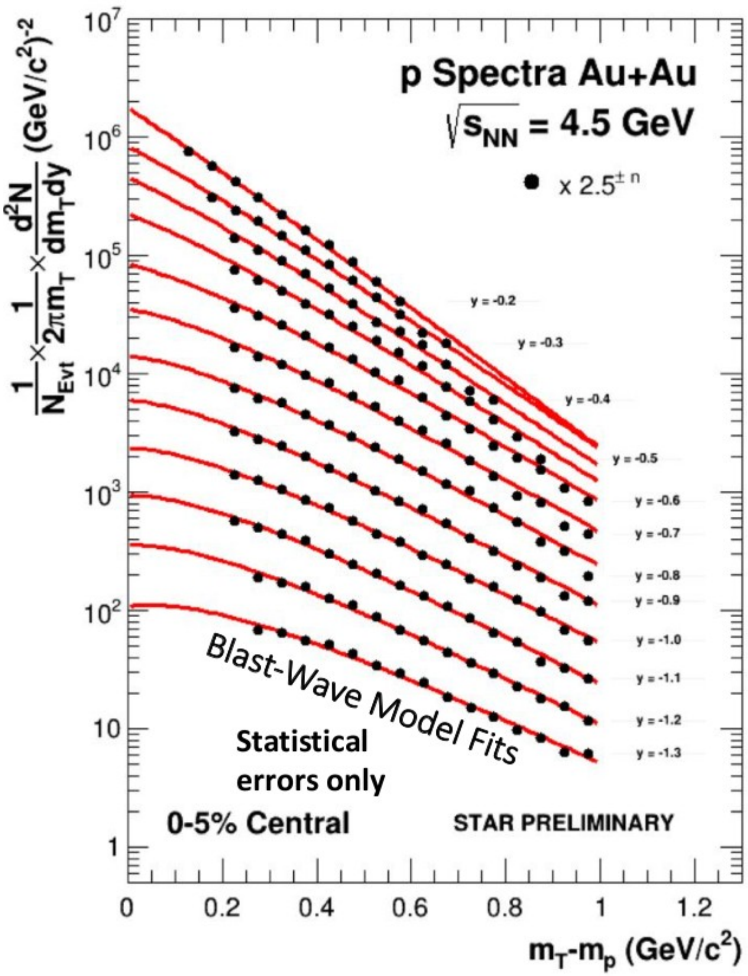

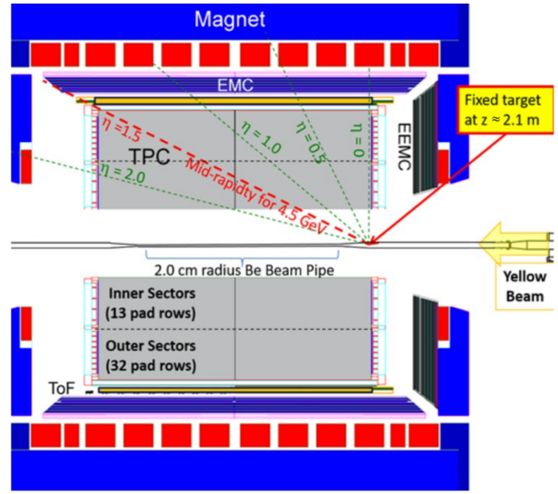

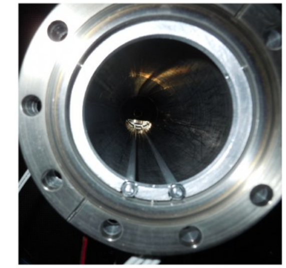

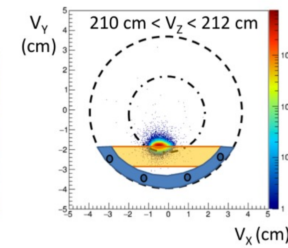

Detector's scheme **(2a)** **(2b)**

Spectra corrections:

Detector efficiency
Detector acceptance
(each rapidity window)
Energy loss

4) Fixed target mode

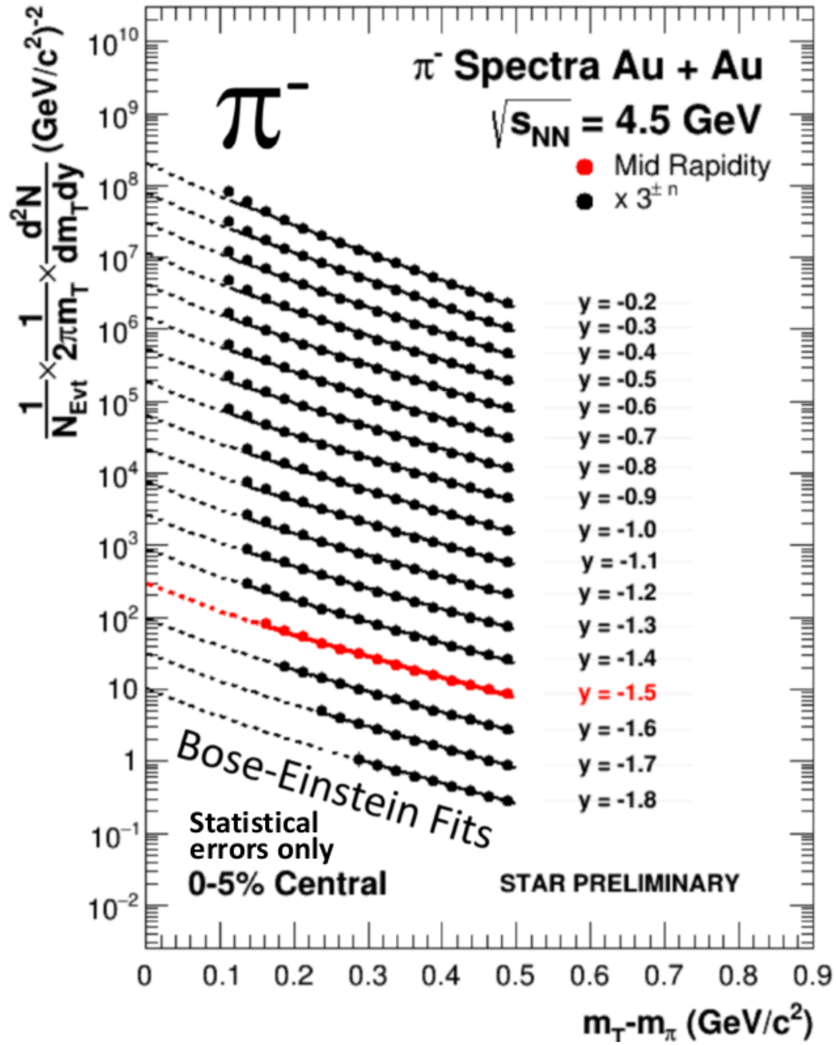

E895 PRC 68 (2003) 054905
E802 PRC 57 (1998) R466
E877 PRC 62 (2000) 024901

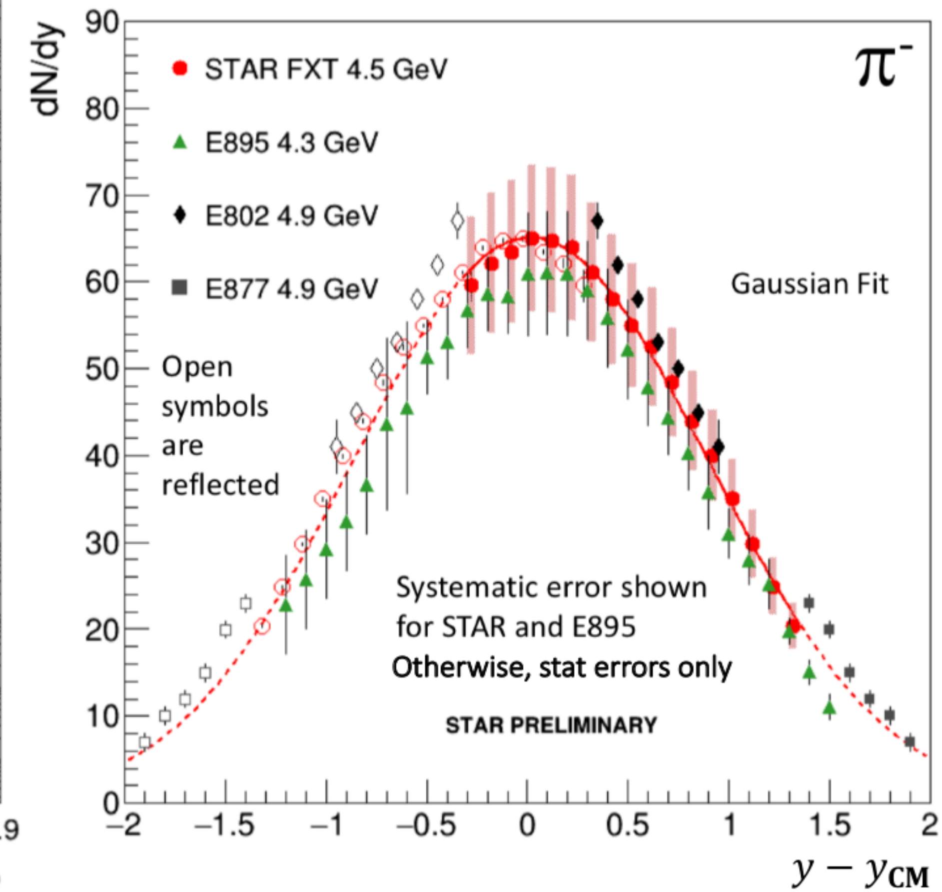

π^- spectra **are consistent** with AGS results.

4) Fixed target mode

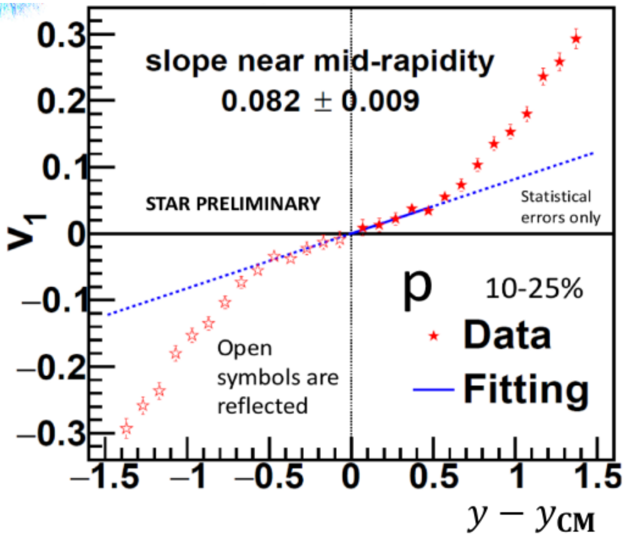

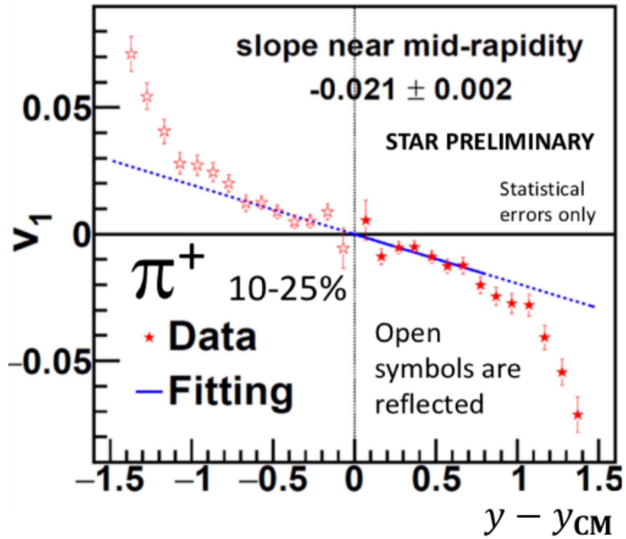

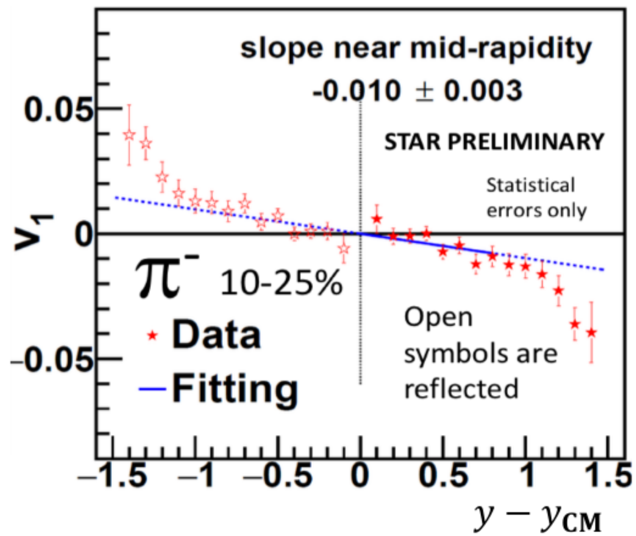

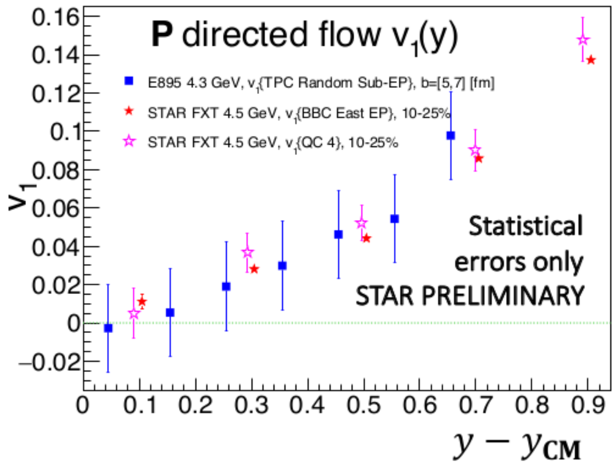

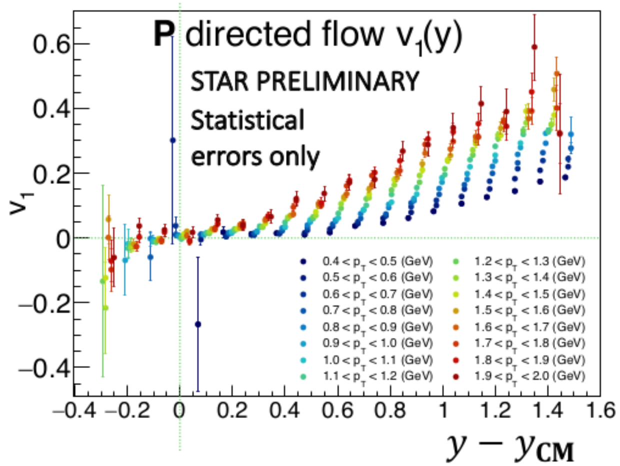

Directed flow for pions and protons with fit describing mid-rapidity region.

Directed flow of protons **agrees** with AGS results.

4) Fixed target mode

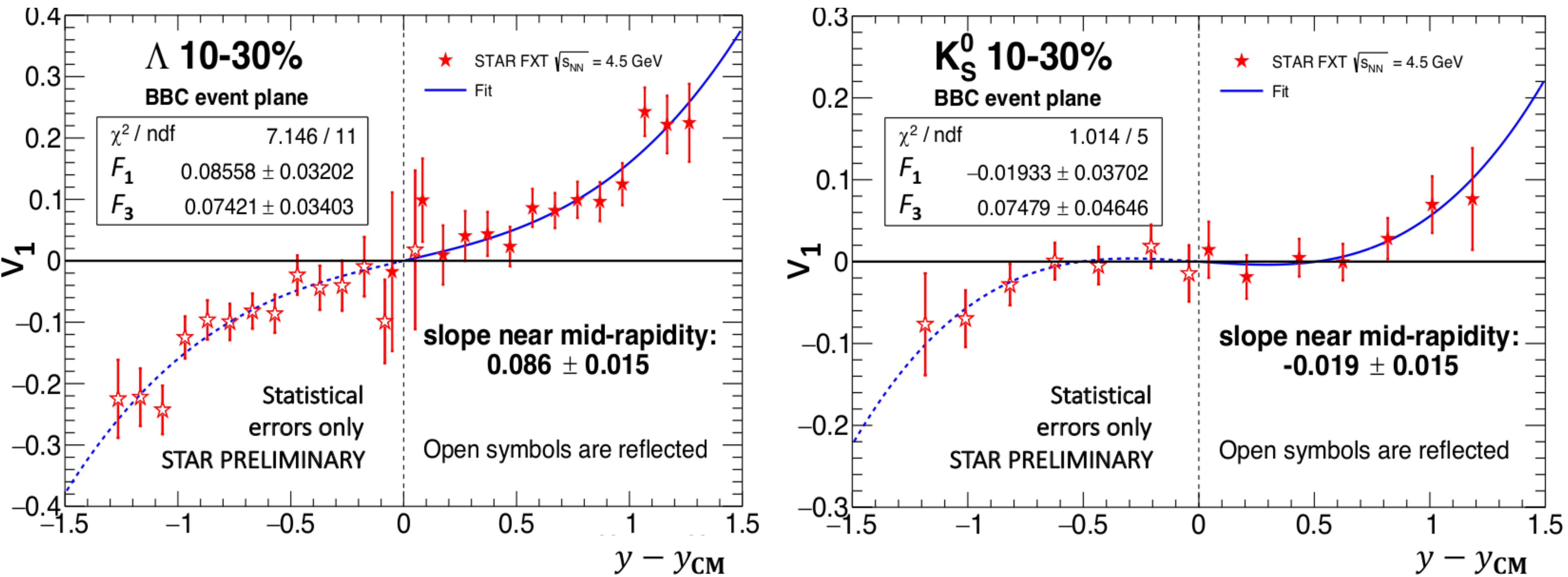

Directed flow for Λ and K^0_S particles and their fits describing mid-rapidity region.

4) Fixed target mode

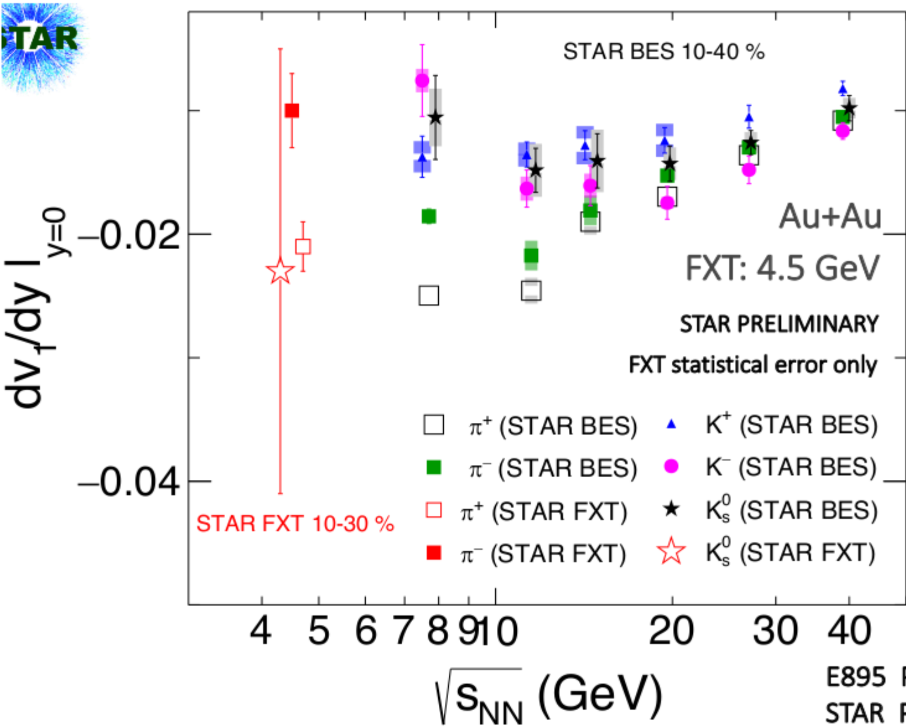

E895 PRL 84 (2000) 5488
STAR PRL 112 (2014) 162301

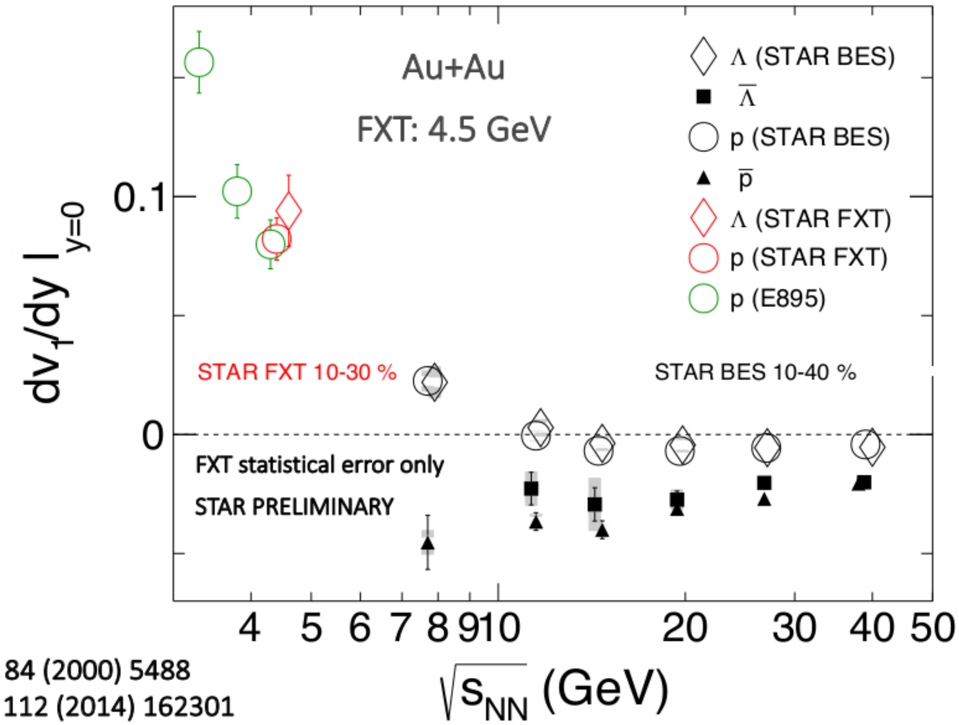

Directed flow for identified particles **agrees** with AGS results.

4) Fixed target mode

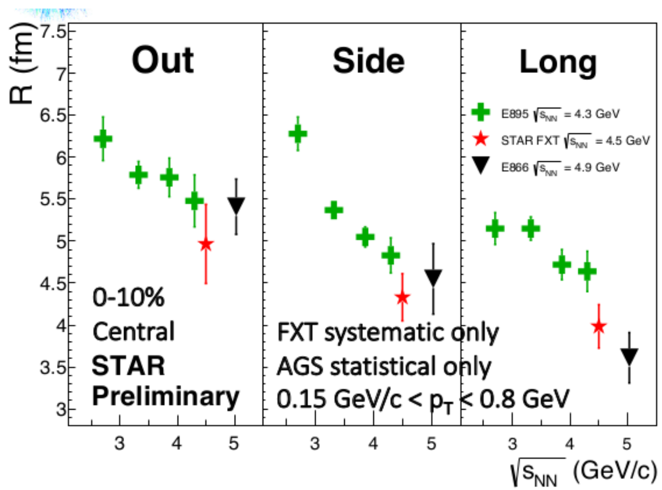

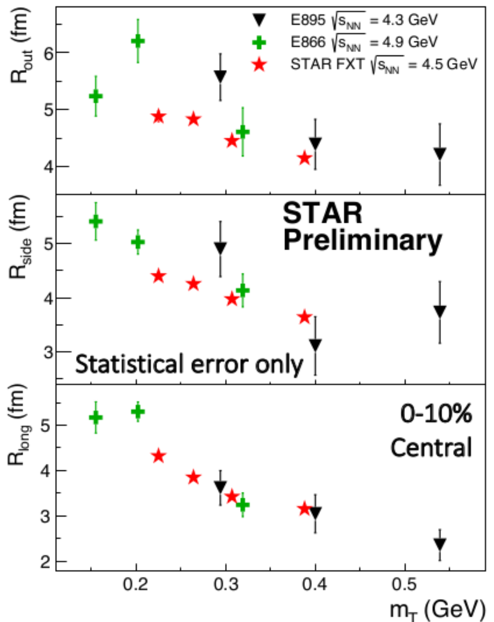

E866 PRC 66 (2002) 054096
E895 PRL 84 (2000) 2798
ALICE PRB 696 (2011) 328
STAR PRC 92 (2015) 14904

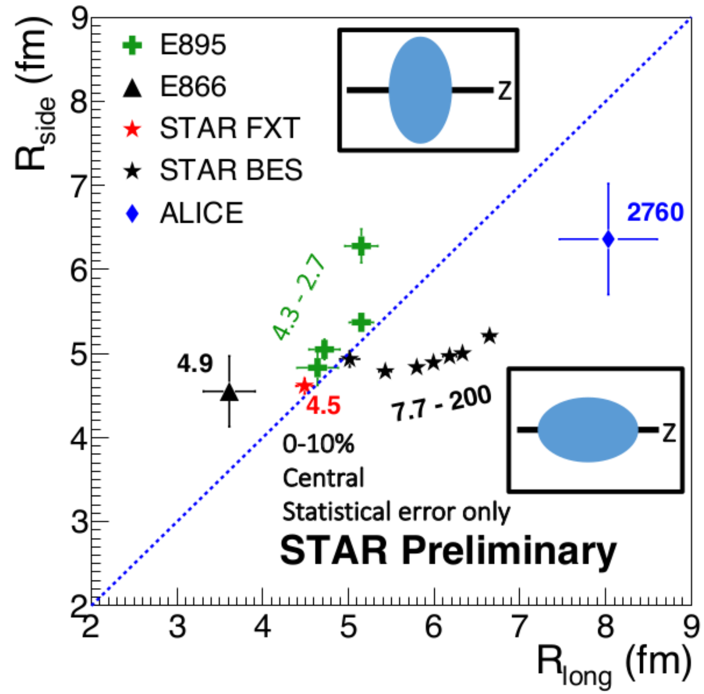

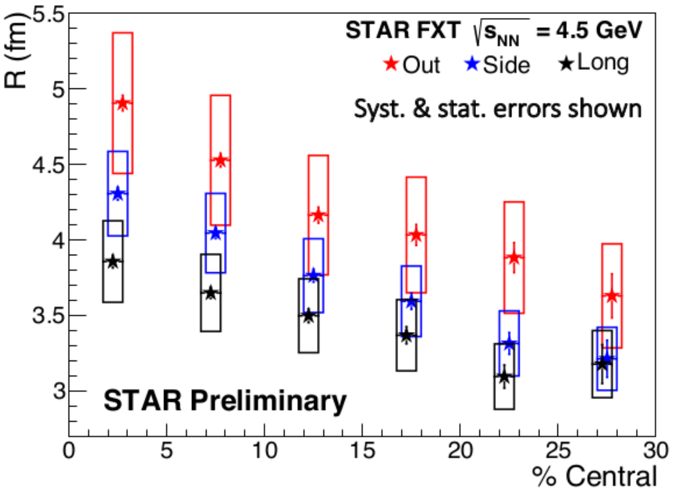

HBT radii for pions are **consistent** with AGS results.

4) Fixed target mode

- **STAR is ready** to operate with the Fixed Target mode

- **Spectra** and **particle yields** agree with AGS results

- **Proton directed flow** and **elliptic flow** (v_1 and v_2) agree with AGS results

- **HBT radii** agree with AGS results

High-baryon density regime will be accessible with the Fix Target mode in STAR!

5) Femtoscopy

Single- and two- particle distributions

$$P_1(p) = E\frac{dN}{d^3p} = \int d^4x\, S(x,p)$$

S(x,p) – emission function: the distribution of source density probability of finding particle with x and p

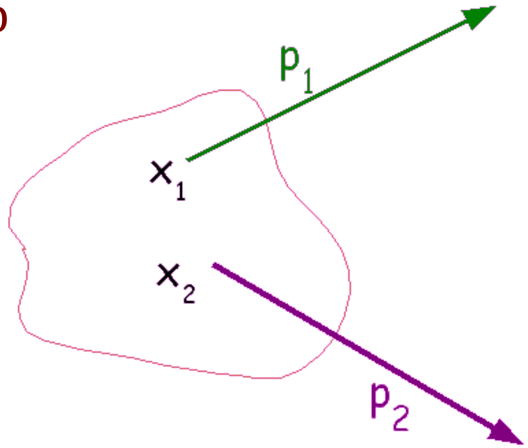

$$P_2(p_1,p_2) = E_1E_2\frac{dN}{d^3p_1d^3p_2} = \int d^4x_1 S(x_1,p_1)\, d^4x_2 S(x_2,p_2)\, \Phi(x_{2,}\, p_2 | x_{1,}\, p_1)$$

The correlation function

$$C(p_1,p_2) = \frac{P_2(p_{1,}\, p_2)}{P_1(p_1)\, P_1(p_2)}$$

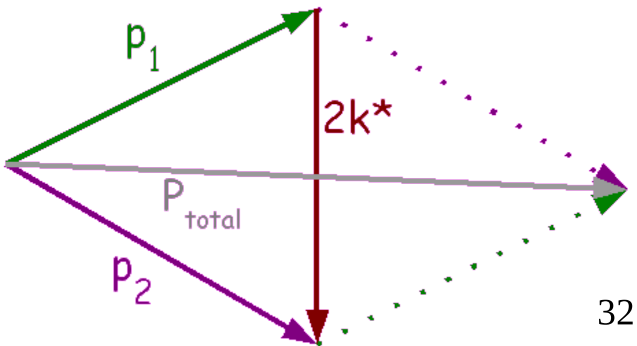

Pair Rest Frame reference

5) Femtoscopy

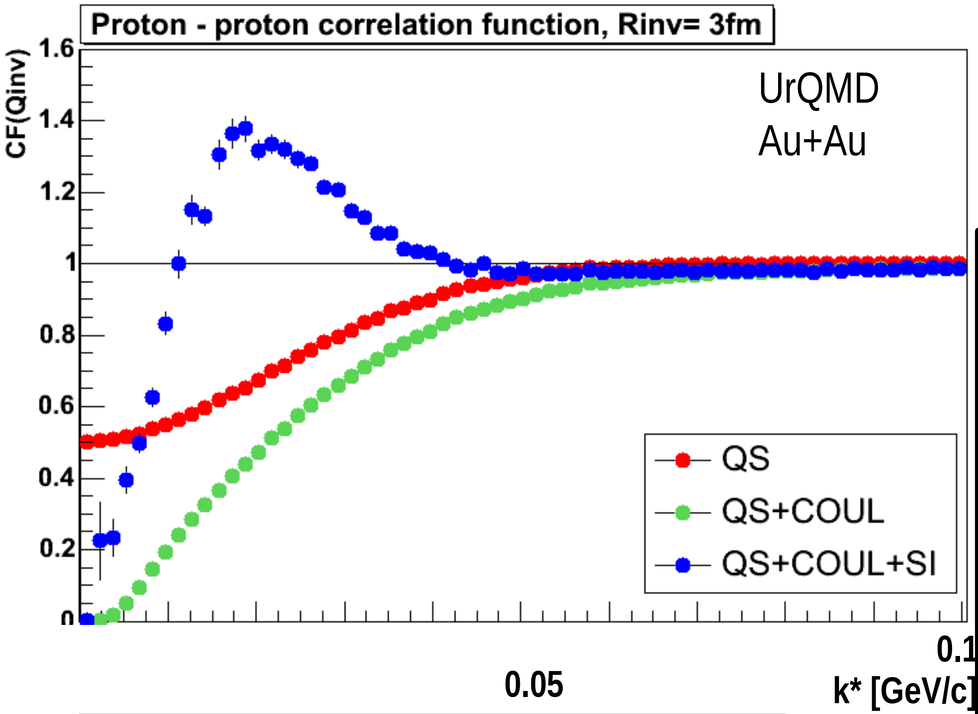

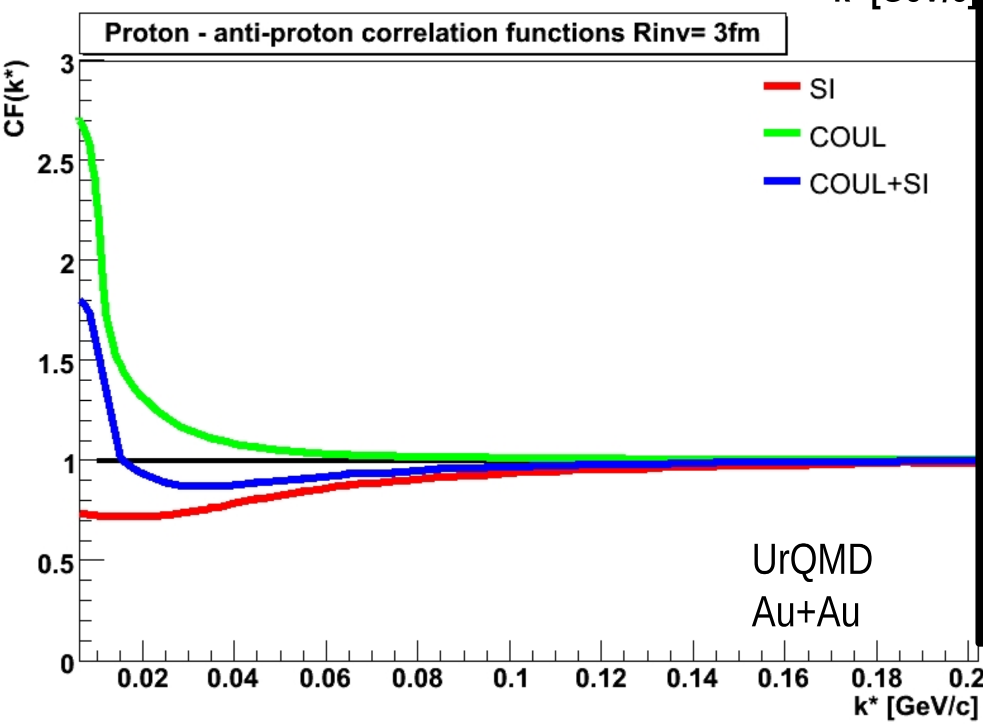

Identical baryon- baryon

- Quantum Statistics- **QS**
- Final State Interactions- **FSI**
  - **Coulomb**
  - **Strong**

Non-identical baryon-(anti)baryon

- Final State Interactions- **FSI**
  - **Coulomb**
  - **Strong**

5) Femtoscopy

proton-proton @39 GeV

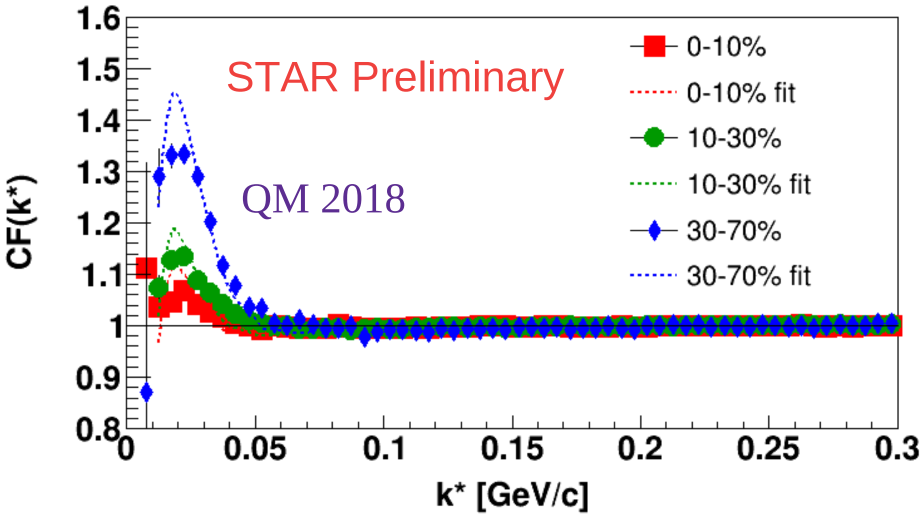

antiproton-antiproton @39 GeV

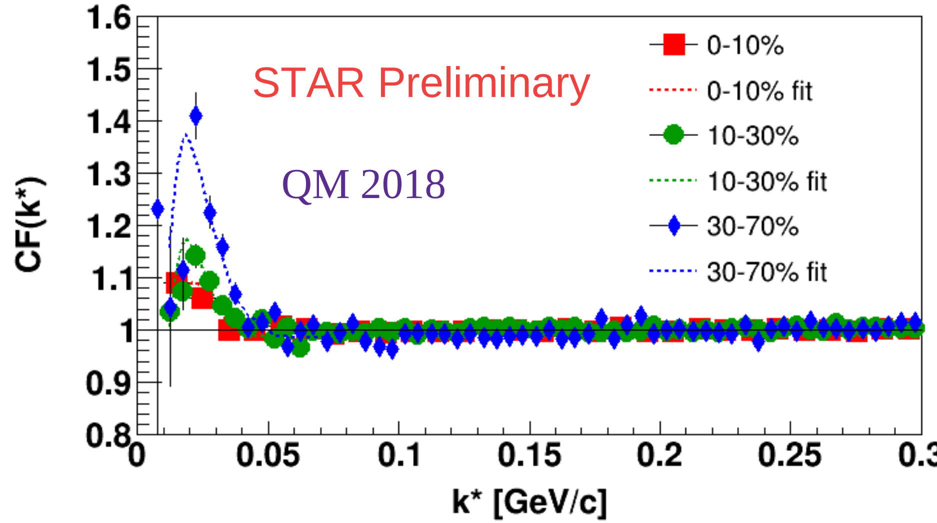

centrality	R_{inv} $p-p$ [fm]	R_{inv} $\overline{p}-\overline{p}$ [fm]	R_{inv} $p-\overline{p}$ [fm]
0-10%	$\mathbf{4.00} \pm 0.15 \pm 0.02$	$\mathbf{3.83} \pm 0.20 \pm 0.03$	$\mathbf{3.39} \pm 0.12 \pm 0.14$
10-30%	$\mathbf{3.61} \pm 0.13 \pm 0.17$	$\mathbf{3.68} \pm 0.15 \pm 0.11$	$\mathbf{2.69} \pm 0.10 \pm 0.12$
30-70%	$\mathbf{2.72} \pm 0.07 \pm 0.07$	$\mathbf{2.95} \pm 0.11 \pm 0.08$	$\mathbf{2.56} \pm 0.09 \pm 0.12$

No significant difference between proton-proton and antiproton-antiproton correlation functions

5) Femtoscopy

Radii from proton-proton and antiproton-antiproton systems differ from those from proton-antiprootn system → Residual Correlations.
Residual feed-down correction needs to be applied.

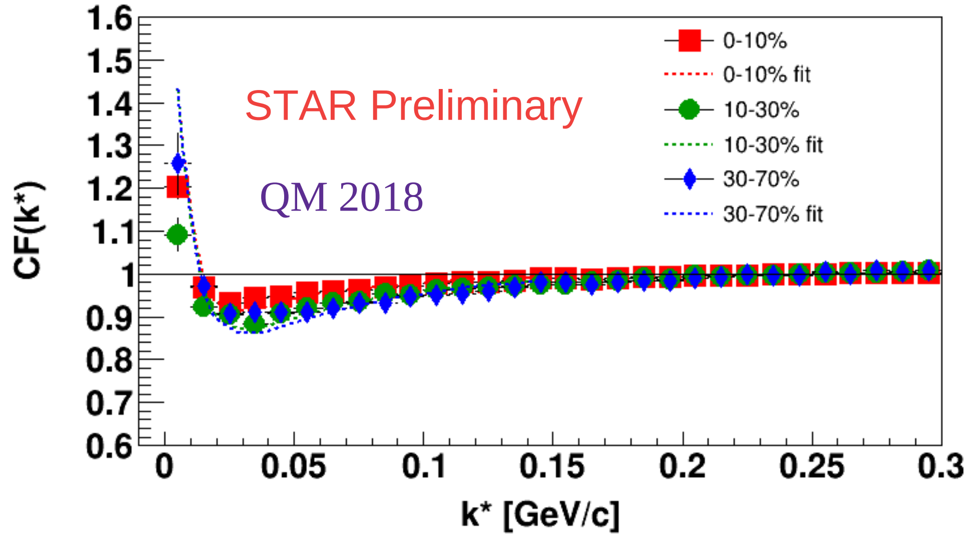

proton-proton @39 GeV

proton-antiproton @39 GeV

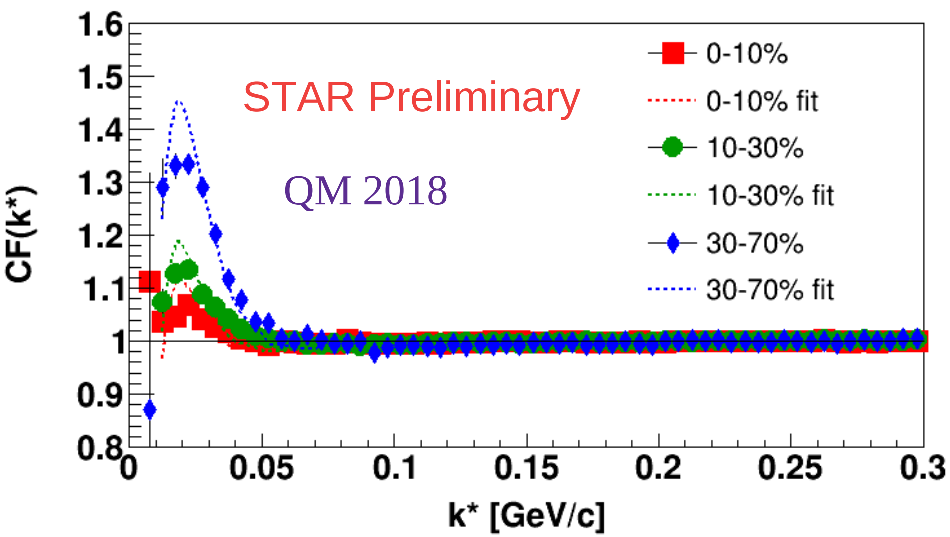

5) Femtoscopy

proton-proton, centrality 0-10%

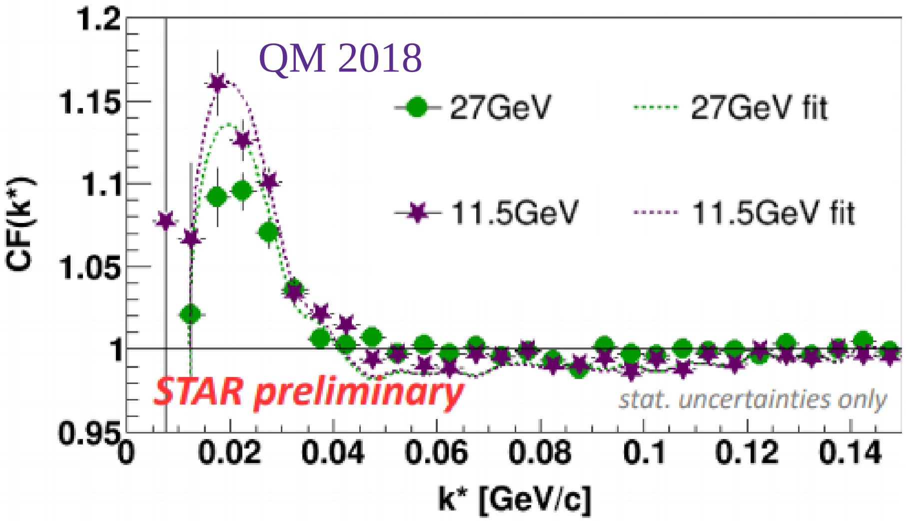

proton-antiproton, centrality 0-10%

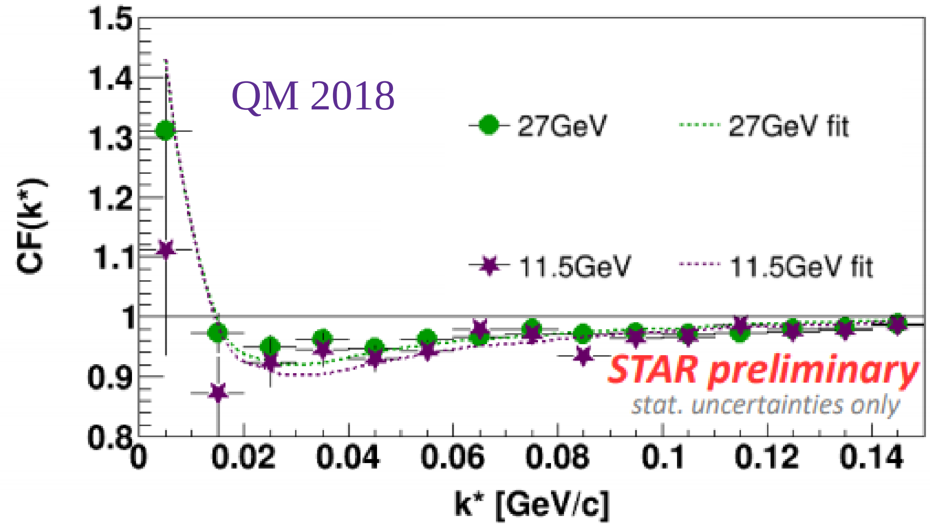

energy	R_{inv} $p-p$ [fm]	R_{inv} $p-\bar{p}$ [fm]
7.7 GeV	$\mathbf{3.59} \pm 0.16 \pm 0.19$	
11.5 GeV	$\mathbf{3.66} \pm 0.08 \pm 0.05$	$\mathbf{3.30} \pm 0.42 \pm 0.28$
19.6 GeV	$\mathbf{3.82} \pm 0.15 \pm 0.06$	$\mathbf{3.32} \pm 0.25 \pm 0.13$
27 GeV	$\mathbf{3.80} \pm 0.12 \pm 0.08$	$\mathbf{3.49} \pm 0.25 \pm 0.16$
39 GeV	$\mathbf{4.00} \pm 0.15 \pm 0.02$	$\mathbf{3.39} \pm 0.12 \pm 0.14$

Energy dependence more significant for proton-proton than for proton-antiproton system.

5) Femtoscopy

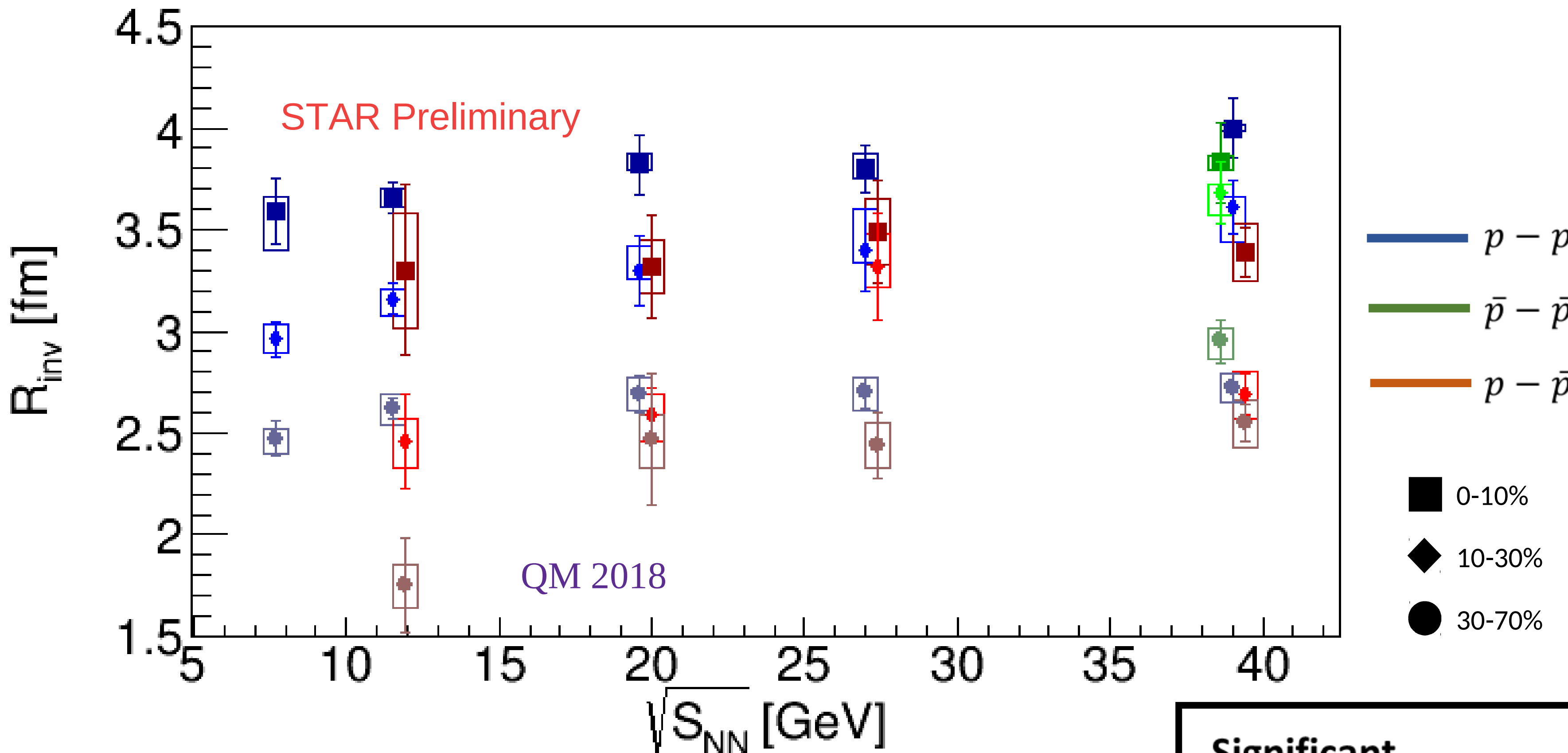

Feed-down correction may decrease significance of centrality dependence.

No significant difference between $p-p$ and $\bar{p}-\bar{p}$ correlation functions at $\sqrt{s_{NN}}$ = 39 GeV

Significant centrality dependence.

$\sqrt{s_{NN}}$ dependence weak for all centralities.

5) Femtoscopy

- Clear centrality dependence of source size at BES energies
- Visible energy dependence of source size at BES energies
- **No visible difference between proton-proton and antiproton-antiproton correlation functions at $\sqrt{s_{NN}}$ = 39 GeV**
- **Correlation functions contaminated by residual correlations – residual correction required**

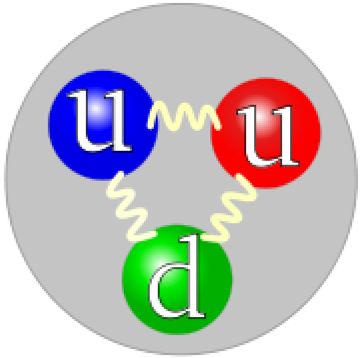

6) Hypertriton

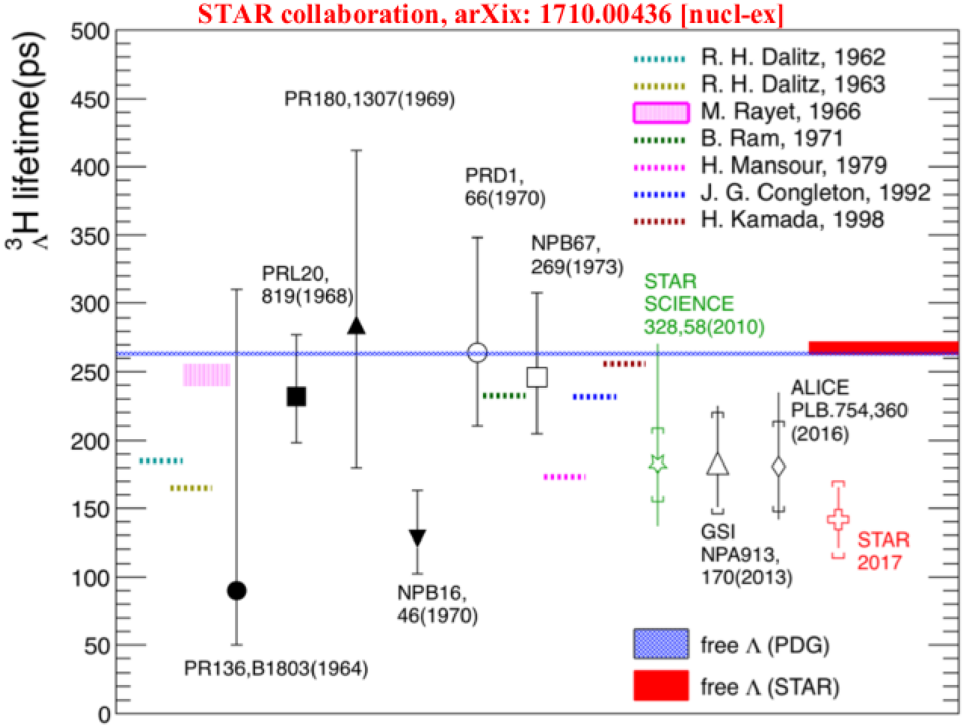

Hyperon-Nucleon:

- play an important role in neutron star and QCD theory

- measurements of masses of hypertriton and anti-hypertriton provide insight into H-N interactions and the CPT symmetry

- measurements sensitive to the temperature and nucleon phase-space of the system freeze-out.

[1] R. O. Gomes, V. Dexheimer, S. Schramm, and C. A. Z. Vasconsellos, The Astrophys. J. 808, 8 (2015).
[2] L. L. Lopes and D. P. Menezes, Phys. Rev. C 89, 025805 (2014).
[3] J. Antoniadis et al., Science 340, 448 (2013).
[4] László P. Csernai, Joseph I. Kapusta, Phys. Reps. 131, 223 (1986).
[5] A. Z. Mekjian, Phys. Rev. C 17, 1051 (1978).
[6] Kaijia Sun et al., Phys. Lett. B 774, 103 (2017).

6) Hypertriton

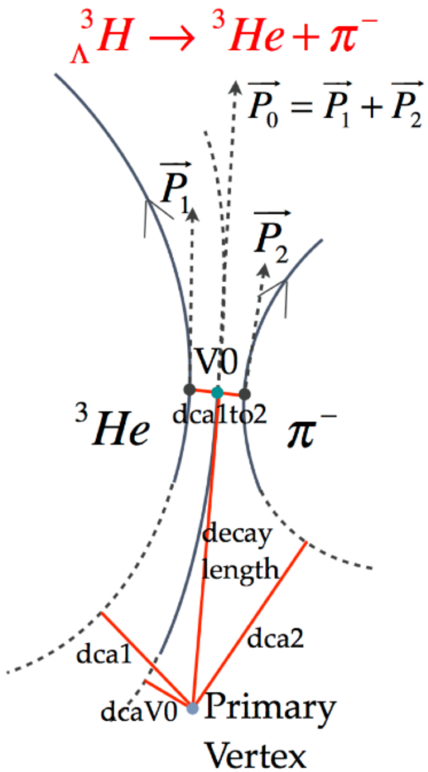

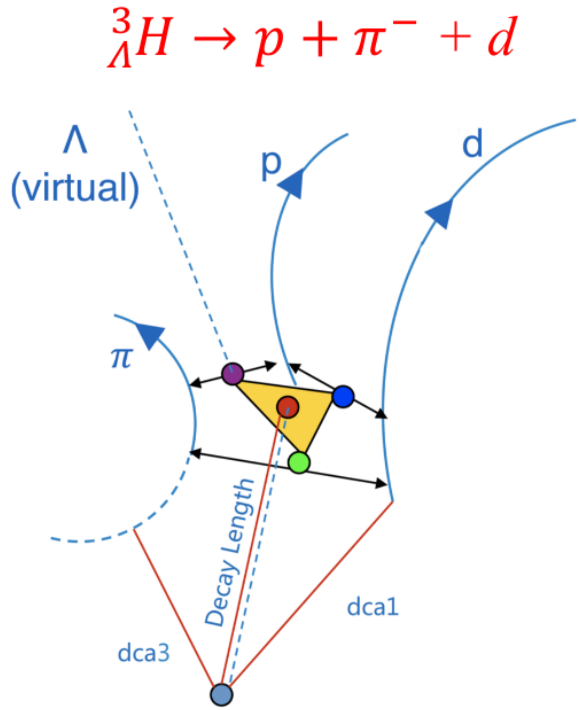

$^3_\Lambda$H has many decay channels:

✓ Non-meson decay channels:

$^3_\Lambda H \to d + n$

$^3_\Lambda H \to p + n + n$

✓ Meson decay channels:

$^3_\Lambda H \to {}^3He\ ({}^3H) + \pi^-\ (\pi^0)$

$^3_\Lambda H \to d + p\ (n) + \pi^-\ (\pi^0)$

$^3_\Lambda H \to p + n + p\ (n) + \pi^-\ (\pi^0)$

Good PID of charged particles in STAR detector.

Reconstructing $^3_\Lambda$H ($^3_{\bar{\Lambda}}\bar{H}$) through:

$^3_\Lambda H \to {}^3He + \pi^-$

$^3_\Lambda H \to d + p + \pi^-$

6) Hypertriton

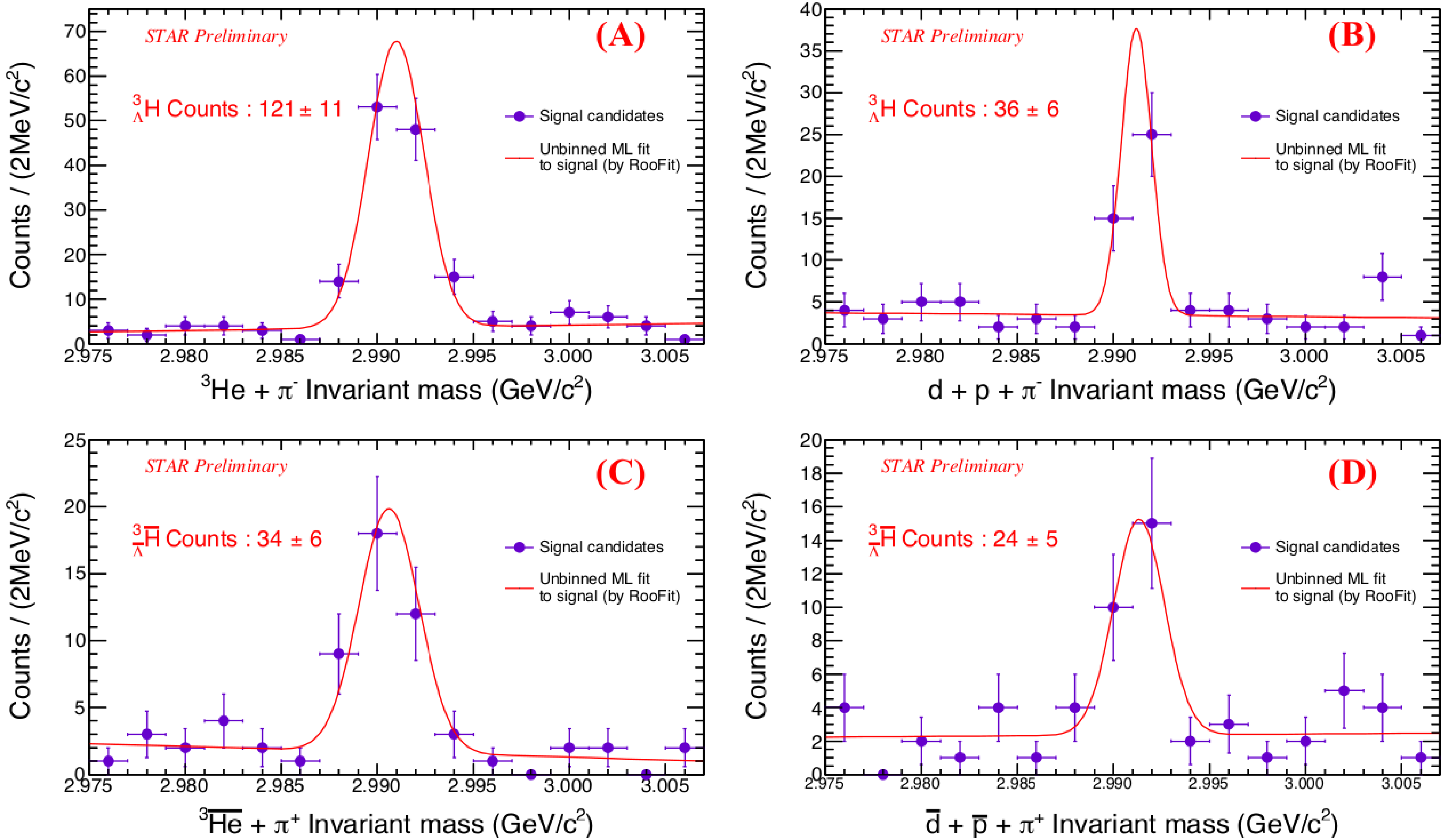

6) Hypertriton

Worldwide binding energy of ${}^{3}_{\Lambda}H$ of experimental measurements.

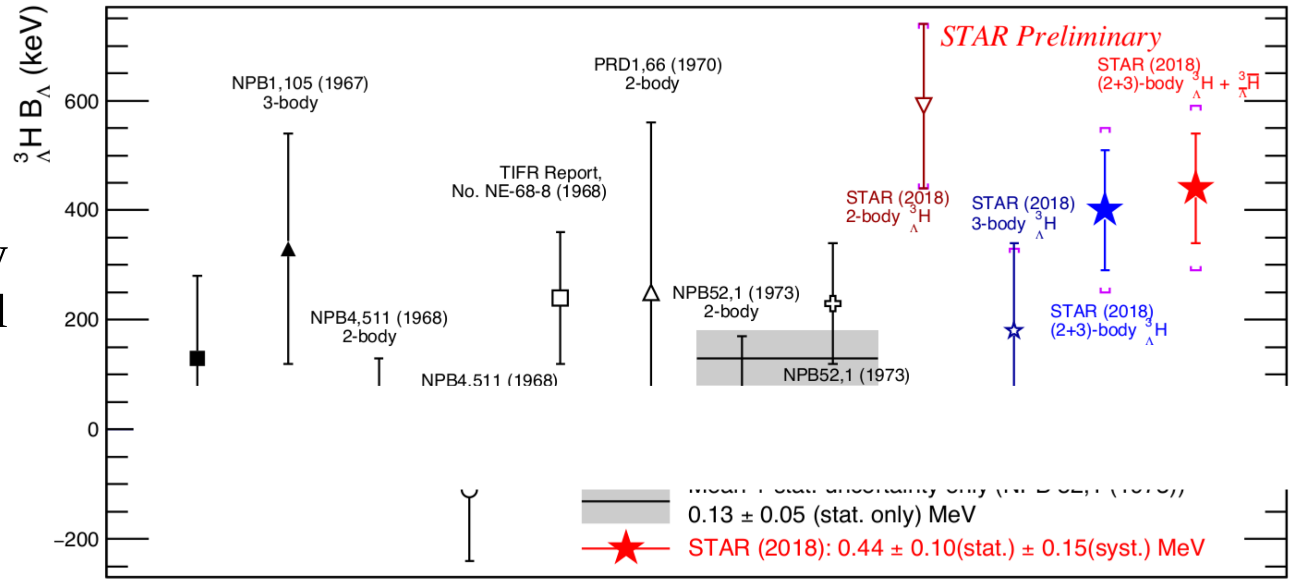

Figure 8. A summary of worldwide binding energy of ${}^{3}_{\Lambda}H$ experimental measurements. The vertical lines are the statistical uncertainty, the brackets are the systematical uncertainty. The gray band is the mean value with its statistical uncertainty measured in 1973.

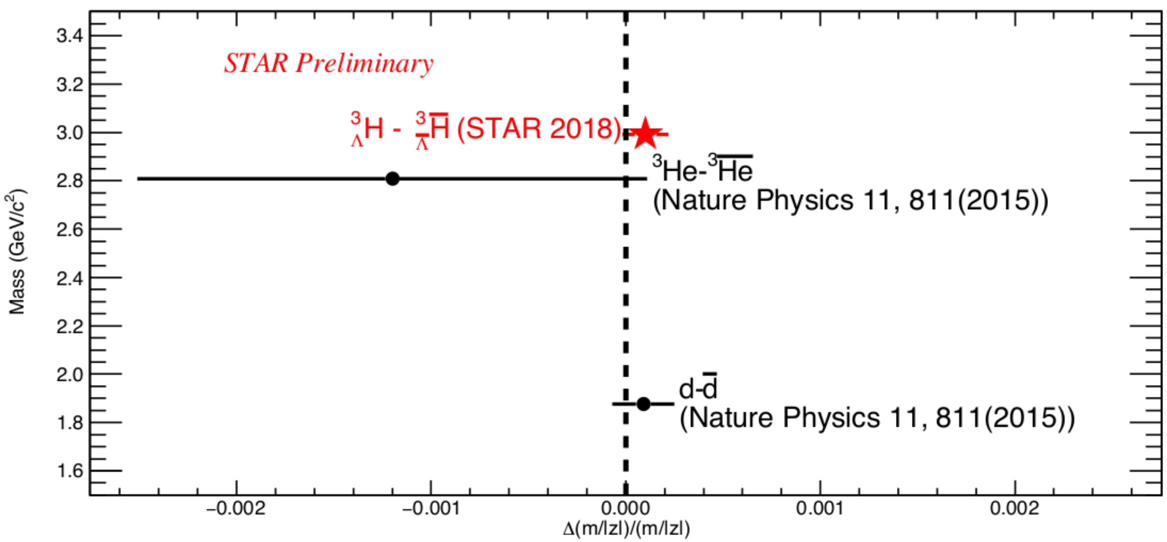

Measurements of the mass-over-charge ratio differences between light nuclei and anti-nuclei.

Conclusions & Summary

Summary

1. Open heavy flavor - D^0 v_1, D^0 R_{AA} and R_{CP}, Λ_C

2. Quarkonium – Υ R_{AA}

3. Jet modification and high-p_T hadrons - di-jet imbalance, di-hadron correlation

4. Chirality, vorticity and polarization effects - Λ polarization, Φ polarization, CME, CMW

5. Initial state physics and approach to equilibrium - v_2 and v_3 fluctuations

6. Collectivity in small systems - v_2 in p+Au and d+Au

7. Collective dynamics - longitudinal decorrelation, identified particle v_1

8. High baryon density and astrophysics - v_1 from fixed target

9. Correlations and fluctuations – femtoscopy

10. Phase diagram and search for the critical point - net Λ and off-diagonal cumulants

11. Thermodynamics and hadron chemistry - triton, hypertriton mass

12. Upgrades - BES-II and forward upgrades

Upgrades

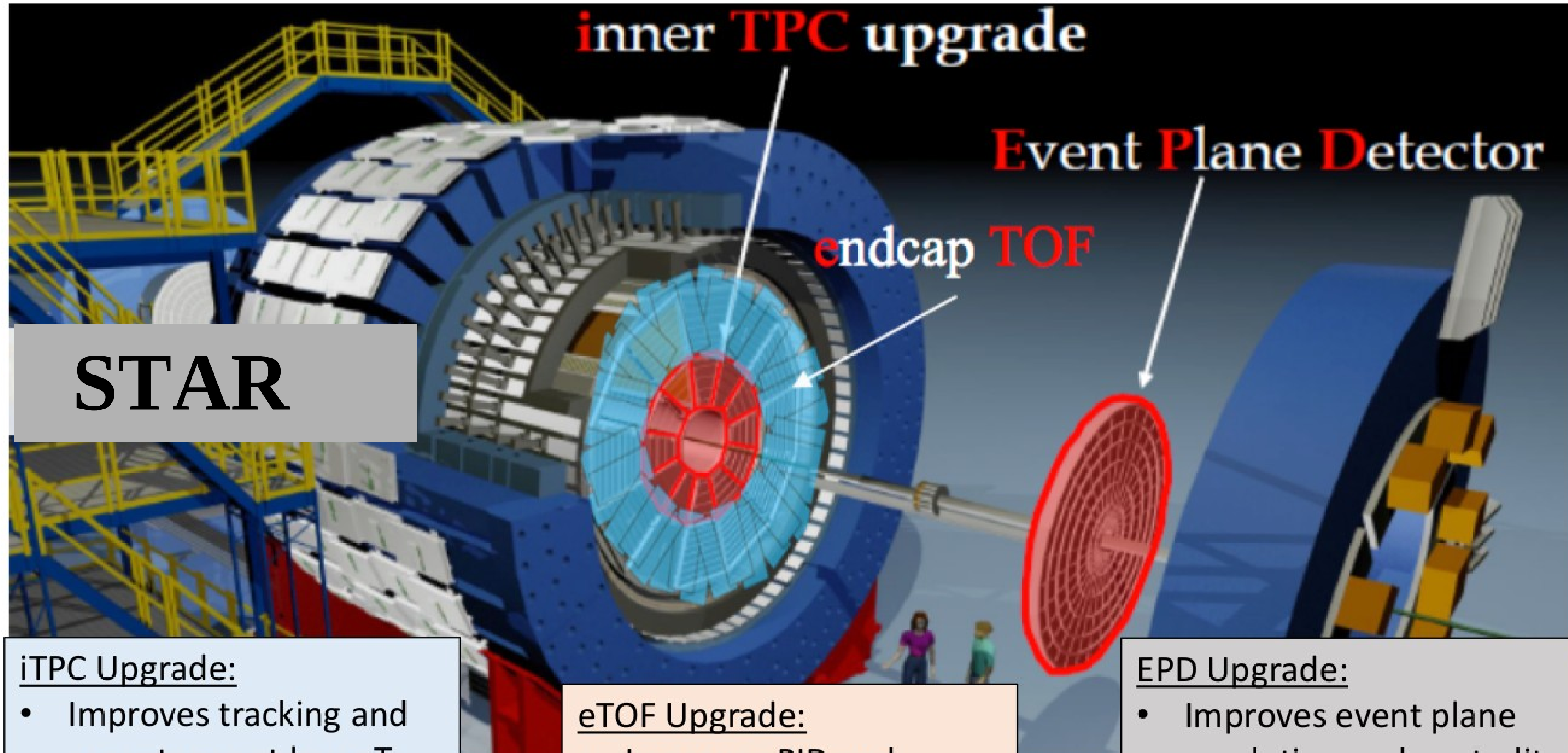

iTPC Upgrade:
- Improves tracking and acceptance at low pT and extra y acceptance
- Ready in 2019

eTOF Upgrade:
- Improves PID and acceptance
- Ready in 2019

EPD Upgrade:
- Improves event plane resolution and centrality definition
- Taking data in 2018 run

STAR Note 0644: Technical Design Report for the iTPC Upgrade

arXiv:1609.05102v1 [nucl-ex]

STAR Note 0666: An Event Plane Detector for STAR

Upgrades

STAR Note 0696: STAR Collaboration Beam Use Request for Run 19+ (Scenario 1)

Single Beam Energy (GeV/nucleon)	$\sqrt{s_{NN}}$ (GeV)	Run Year	Run Time	Species	Min-Bias Events Number
5.75	3.5 (FXT)	2020	2 days	Au+Au	100M
7.3	3.9 (FXT)	2019	2 days	Au+Au	100M
9.8	4.5 (FXT)	2019	2 days	Au+Au	100M
13.5	5.2 (FXT)	2020	2 days	Au+Au	100M
19.5	6.2 (FXT)	2020	2 days	Au+Au	100M
31.2	7.7 (FXT)	2019	2 days	Au+Au	100M

- iTPC & eTOF upgrades will be available
- Need 100M events at each energy to match sensitivity of BES-II: 2 days per energy (3.5 GeV – 7.7 GeV)
- Data rate is DAQ limited
- Data at 7.7 GeV will provide an overlap energy with collider mode

FXT in Run 18

Trigger commissioning occurring now

1 Billion events at 7.2 GeV

100 Million events at 3.0 GeV

EPD ready and available for flow analyses

Can obtain fluctuation measurement at energies below BES-I

Thank you!

6) Hipertriton

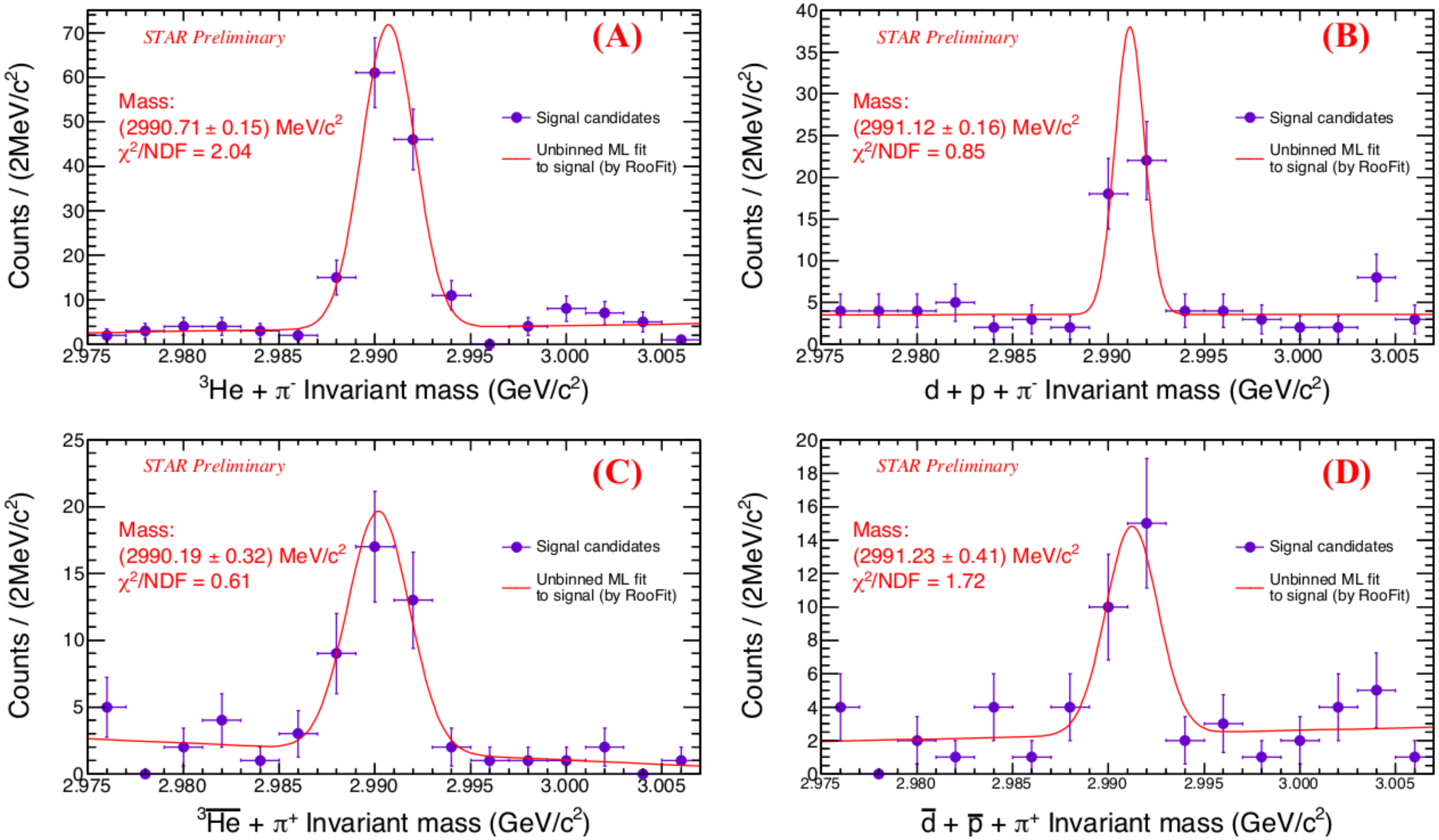

Energy loss in the material in front of and in the TPC.

$^3_\Lambda$H (2-body + 3-body)
2990.90 $\pm$ 0.11 (stat.) $\pm$ 0.15 (syst.) MeV/c^2

$^3_{\bar{\Lambda}}\bar{\text{H}}$ (2-body + 3-body)
2990.59 $\pm$ 0.25 (stat.) $\pm$ 0.15 (syst.) MeV/c^2

$^3_\Lambda$H and $^3_{\bar{\Lambda}}\bar{\text{H}}$ combined
2990.85 $\pm$ 0.10 (stat.) $\pm$ 0.15 (syst.) MeV/c^2

Systematical uncertainty source:

- **Energy loss correction.**
- **Different cuts impact.**

Fit Function:

$$N_{sig}\left(\frac{1}{\sqrt{2\pi\sigma^2}}e^{-\frac{(x-\mu)^2}{2\sigma^2}}\right) + N_{bkg}(ax+b)$$

6) Hipertriton

Hypertriton B_Λ definition:

$m_\Lambda + m_d - m_{^3_\Lambda H}$

1. Early measurements of B_Λ have large statistical uncertainty due to the limited statistics.

2. The difference between the STAR measurement and the previous measurement is 0.31 ± 0.11 (stat. only) MeV.

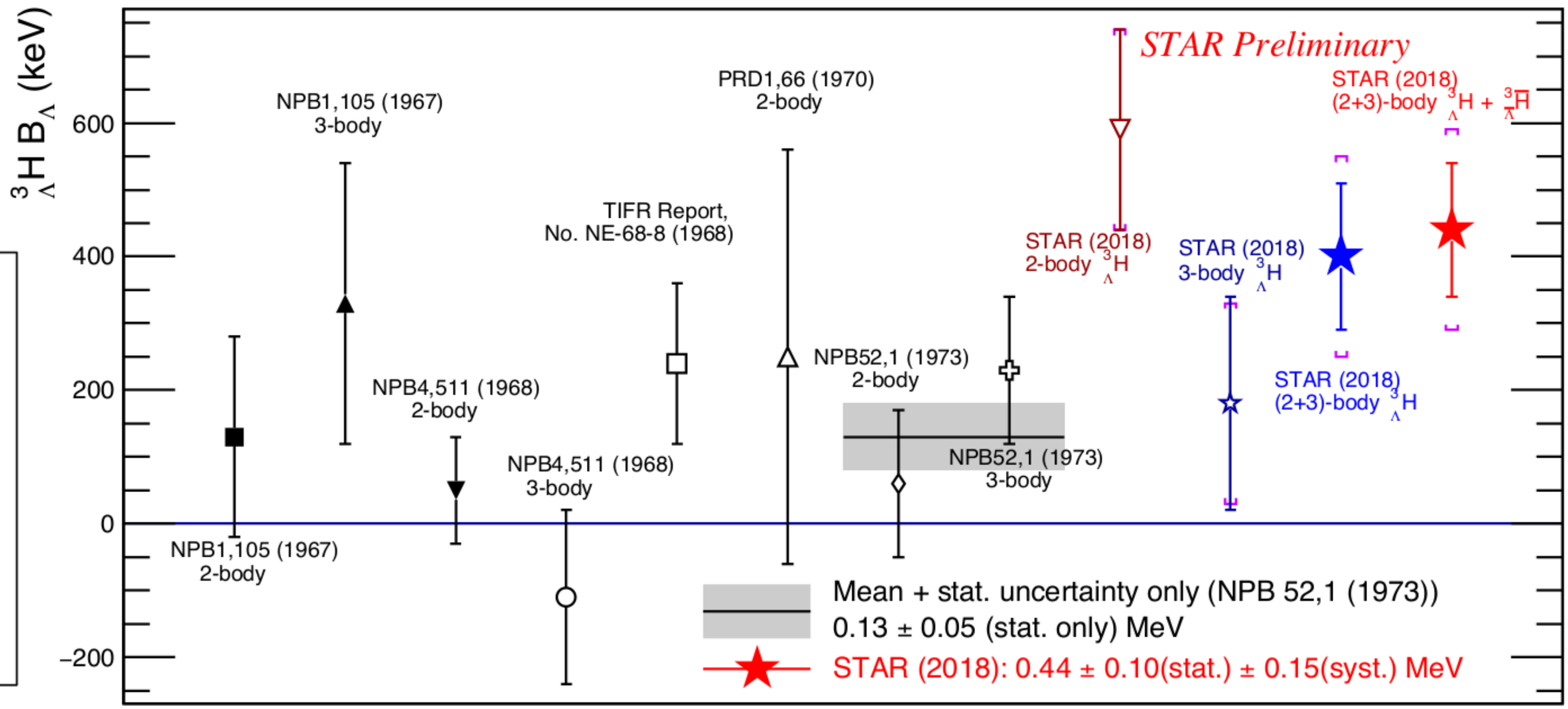

Figure 8. A summary of worldwide binding energy of $^3_\Lambda$H experimental measurements. The vertical lines are the statistical uncertainty, the brackets are the systematical uncertainty. The gray band is the mean value with its statistical uncertainty measured in 1973.

6) Hipertriton

1. ${}^{3}_{\Lambda}H$ was discovered in 1952.

2. ${}^{3}_{\Lambda}\overline{H}$ was discovered in 2010 by STAR collaboration [7].

3. Mass difference between ${}^{3}_{\Lambda}H$ and ${}^{3}_{\Lambda}\overline{H}$ was measured for the first time.

4. The mass difference consistent with CPT prediction.

5. Test of CPT symmetry in the light hypernuclei sector.

$$\left(\frac{\Delta(m/|z|)}{m/|z|}\right)_{d} = (0.9 \pm 0.5\,(\text{stat.}) \pm 1.4\,(\text{syst.}))\times 10^{-4}$$

$$\left(\frac{\Delta(m/|z|)}{m/|z|}\right)_{{}^{3}He} = (-1.2 \pm 0.9\,(\text{stat.}) \pm 1.0\,(\text{syst.}))\times 10^{-3}$$

$$\left(\frac{\Delta m}{m}\right)_{{}^{3}_{\Lambda}H} = (1.0 \pm 0.9\,(\text{stat.}) \pm 0.7\,(\text{syst.}))\times 10^{-4}$$

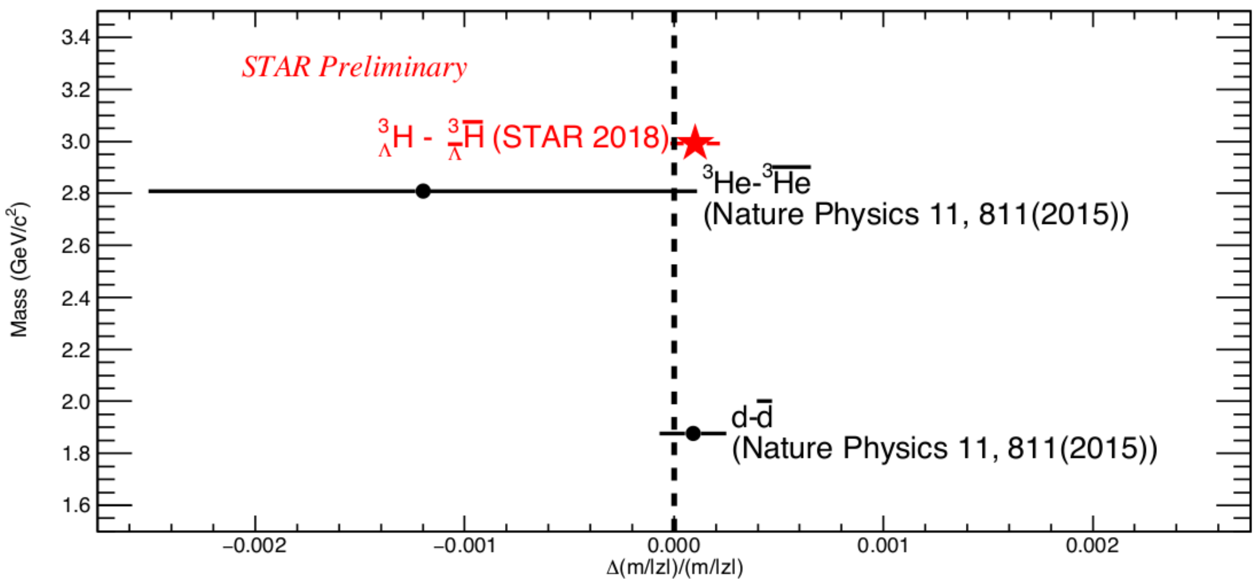

[7] B. I. Abelev et al. (STAR Collaboration), Science 328, 58 (2010).

6) Hipertriton